

This is an Open Access document downloaded from ORCA, Cardiff University's institutional repository: <https://orca.cardiff.ac.uk/id/eprint/161120/>

This is the author's version of a work that was submitted to / accepted for publication.

Citation for final published version:

Shao, Yong, Zhou, Long, Li, Fang, Zhao, Lan, Zhang, Bao-Lin, Shao, Feng, Chen, Jia-Wei, Chen, Chun-Yan, Bi, Xupeng, Zhuang, Xiao-Lin, Zhu, Hong-Liang, Hu, Jiang, Sun, Zongyi, Li, Xin, Wang, Depeng, Rivas-González, Iker, Wang, Sheng, Wang, Yun-Mei, Chen, Wu, Li, Gang, Lu, Hui-Meng, Liu, Yang, Kuderna, Lukas F. K., Farh, Kyle Kai-How, Fan, Peng-Fei, Yu, Li, Li, Ming, Liu, Zhi-Jin, Tiley, George P., Yoder, Anne D., Roos, Christian, Hayakawa, Takashi, Marques-Bonet, Tomas, Rogers, Jeffrey, Stenson, Peter D., Cooper, David N., Schierup, Mikkel Heide, Yao, Yong-Gang, Zhang, Ya-Ping, Wang, Wen, Qi, Xiao-Guang, Zhang, Guojie and Wu, Dong-Dong 2023. Phylogenomic analyses provide insights into primate evolution. *Science* 380 (6648) , pp. 913-924. 10.1126/science.abn6919

Publishers page: <http://dx.doi.org/10.1126/science.abn6919>

Please note:

Changes made as a result of publishing processes such as copy-editing, formatting and page numbers may not be reflected in this version. For the definitive version of this publication, please refer to the published source. You are advised to consult the publisher's version if you wish to cite this paper.

This version is being made available in accordance with publisher policies. See <http://orca.cf.ac.uk/policies.html> for usage policies. Copyright and moral rights for publications made available in ORCA are retained by the copyright holders.



1 **Title: Phylogenomic analyses provide insights into primate evolution**

2

3 **Authors:** Yong Shao ^{1*}, Long Zhou ^{2*}, Fang Li ^{3,4}, Lan Zhao ⁵, Bao-Lin Zhang ¹, Feng Shao
4 ⁶, Jia-Wei Chen ⁷, Chun-Yan Chen ⁸, Xu-Peng Bi ², Xiao-Lin Zhuang ^{1,9}, Hong-Liang Zhu ⁷,
5 Jiang Hu ¹⁰, Zongyi Sun ¹⁰, Xin Li ¹⁰, Depeng Wang ¹⁰, Iker Rivas-González ¹¹, Sheng Wang ¹,
6 Yun-Mei Wang ¹, Wu Chen ¹², Gang Li ¹³, Hui-Meng Lu ¹⁴, Yang Liu ¹³, Lukas Kuderna ¹⁵,
7 Kyle Kai-How Farh ¹⁶, Peng-Fei Fan ¹⁷, Li Yu ¹⁸, Ming Li ¹⁹, Zhi-Jin Liu ²⁰, George P Tiley ²¹,
8 Anne D Yoder ²¹, Christian Roos ²², Takashi Hayakawa ^{23,24}, Tomas Marques-Bonet ^{15,25},
9 Jeffrey Rogers ²⁶, Peter D Stenson ²⁷, David N. Cooper ²⁷, Mikkel Heide Schierup ¹¹, Yong-
10 Gang Yao ^{9,28,29,30}, Ya-Ping Zhang ^{1,29,30}, Wen Wang ^{1,8,29}, Xiao-Guang Qi ^{5,†}, Guojie Zhang ^{1,}
11 ^{2,3,31,†}, Dong-Dong Wu ^{1,29,30,32,†}

12

13 **Affiliations:**

- 14 1. State Key Laboratory of Genetic Resources and Evolution, Kunming Natural History
15 Museum of Zoology, Kunming Institute of Zoology, Chinese Academy of Sciences,
16 Kunming, 650201, China.
- 17 2. Center of Evolutionary & Organismal Biology, and Women's Hospital at
18 Zhejiang University School of Medicine, Hangzhou, 310058, China
- 19 3. Section for Ecology and Evolution, Department of Biology, University of Copenhagen,
20 Copenhagen, DK-2100, Denmark
- 21 4. Institute of Animal Sex and Development, Zhejiang Wanli University, Ningbo, China
- 22 5. Shaanxi Key Laboratory for Animal Conservation, College of Life Sciences, Northwest
23 University, Xi'an, China
- 24 6. Key Laboratory of Freshwater Fish Reproduction and Development (Ministry of
25 Education), Southwest University School of Life Sciences, Chongqing 400715, China
- 26 7. BGI-Shenzhen, Shenzhen 518083, China
- 27 8. School of Ecology and Environment, Northwestern Polytechnical University, Xi'an,
28 710072, China
- 29 9. Kunming College of Life Science, University of the Chinese Academy of Sciences,
30 Kunming, 650204, China
- 31 10. Grandomics Biosciences, Beijing 102206, China
- 32 11. Bioinformatics Research Centre, Aarhus University, Aarhus C., DK-8000, Denmark
- 33 12. Guangzhou Zoo & Guangzhou Wildlife Research Center, Guangzhou, 510070, China
- 34 13. College of Life Sciences, Shaanxi Normal University, Xi'an, China
- 35 14. School of Life Sciences, Northwestern Polytechnical University, Xi'an, China
- 36 15. Institute of Evolutionary Biology (UPF-CSIC), PRBB, Dr. Aiguader 88, 08003
37 Barcelona, Spain
- 38 16. Illumina Artificial Intelligence Laboratory, Illumina Inc, San Diego, CA, USA
- 39 17. School of Life Sciences, Sun Yat-sen University, Guangzhou, Guangdong 510275, China
- 40 18. State Key Laboratory for Conservation and Utilization of Bio-Resource in Yunnan,
41 School of Life Sciences, Yunnan University, Kunming, China
- 42 19. CAS Key Laboratory of Animal Ecology and Conservation Biology, Institute of
43 Zoology, Chinese Academy of Sciences, Beijing 100101, China
- 44 20. College of Life Sciences, Capital Normal University, Beijing 100048, China

- 45 21. Department of Biology, Duke University, Durham, NC 27708, USA
46 22. Gene Bank of Primates and Primate Genetics Laboratory, German Primate Center,
47 Leibniz Institute for Primate Research, Göttingen 37077, Germany
48 23. Faculty of Environmental Earth Science, Hokkaido University, Sapporo, Hokkaido 060-
49 0810, Japan
50 24. Japan Monkey Centre, Inuyama, Aichi 484-0081, Japan
51 25. Institut de Biologia Evolutiva, Pompeu Fabra University and Spanish National Research
52 Council, 08003 Barcelona, Spain
53 26. Human Genome Sequencing Center, Department of Molecular and Human Genetics,
54 Baylor College of Medicine, Houston, TX 77030, USA
55 27. Institute of Medical Genetics, School of Medicine, Cardiff University, Cardiff, CF14
56 4XN, UK
57 28. Key Laboratory of Animal Models and Human Disease Mechanisms of Chinese
58 Academy of Sciences & Yunnan Province, Kunming Institute of Zoology, Chinese
59 Academy of Sciences, Kunming, Yunnan, 650201, China
60 29. Center for Excellence in Animal Evolution and Genetics, Chinese Academy of Sciences,
61 Kunming, Yunnan 650223, China
62 30. National Resource Center for Non-Human Primates, Kunming Primate Research Center,
63 and National Research Facility for Phenotypic & Genetic Analysis of Model Animals
64 (Primate Facility), Kunming Institute of Zoology, Chinese Academy of Sciences,
65 Kunming, Yunnan 650107, China
66 31. Liangzhu Laboratory, Zhejiang University Medical Center, 1369 West Wenyi Road,
67 Hangzhou 311121, China
68 32. KIZ-CUHK Joint Laboratory of Bioresources and Molecular Research in Common
69 Diseases, Kunming Institute of Zoology, Chinese Academy of Sciences, Kunming
70 650204, China

71

72 *These authors contributed equally to this work.

73 †Corresponding authors:

74 Dong-Dong Wu: wudongdong@mail.kiz.ac.cn;

75 Guojie Zhang: guojiezhang@zju.edu.cn;

76 Xiao-Guang Qi: qixg@nwu.edu.cn.

77

78 **Abstract**

79 Comparative analysis of primate genomes within a phylogenetic context is essential for
80 understanding the evolution of human genetic architecture and primate diversity. We present
81 such a study of 50 primate species spanning 38 genera and 14 families, including 27 genomes
82 first reported here, with many from previously less well represented groups, the New World
83 monkeys and the Strepsirrhini. Our analyses reveal heterogeneous rates of genomic
84 rearrangement and gene evolution across primate lineages. Thousands of genes under positive
85 selection in different lineages play roles in the nervous, skeletal and digestive systems and
86 may have contributed to primate innovations and adaptations. Our study reveals that many
87 key genomic innovations occurred in the Simiiformes ancestral node and may have had an
88 impact on the adaptive radiation of the Simiiformes and human evolution.

89

90 **One-Sentence Summary:** Comparative genomics reconstructs the evolutionary processes
91 within the primates.

92

93 **Main text**

94 The order Primates contains more than 500 species from 79 genera and 16 families (*1*), with
95 new primate species continuing to be discovered (2-5), making primates the third most
96 speciose order of living mammals after bats (Chiroptera) and rodents (Rodentia). As our
97 closest living relatives, non-human primates play important roles in the cultures and religions
98 of human societies (*1*). Many non-human primate species have been widely used as animal
99 models, on the basis of their genetic, physiological and anatomical similarities to humans, to
100 allow the efficacy and safety of newly developed drugs and vaccines to be tested (6). For
101 example, since the emergence of COVID19, macaques have served as important models in
102 the research and development of vaccines (7-16). Primates display considerable
103 morphological, behavioural and physiological diversity, and hold the key to understanding the
104 evolution of our own species, particularly the evolution of human phenotypes such as high
105 level cognition (*17, 18*).

106

107 Non-human primates occupy a wide range of diverse habitats in the tropical forests, savanna,
108 semi-desert and subtropical regions of Asia, Central and South America, and Africa, whilst
109 humans have spread across much of the earth's surface. Nevertheless, according to the
110 International Union for Conservation of Nature (IUCN) Red Lists, more than a third of
111 primate species are critically endangered or vulnerable, about 60% of primate species are
112 threatened with extinction, while 75% of primate species are experiencing population decline
113 (*1*). With global climate change and increasing anthropogenic interference, the conservation
114 status of primates has attracted global scientific and public awareness.

115

116 Despite their importance, reference genomes have been sequenced in fewer than 10% of non-
117 human primate species (*19-27*), a state of affairs that both impedes research and hampers
118 conservation efforts. Here we present high quality reference genomes for 27 primate species
119 with long read sequencing generated from our first phase program of the Primate Genome
120 Project.

121

122 **Assembly and annotation of 27 new primate reference genomes**

123 We applied long-read genome sequencing technologies, including Pacbio and Nanopore, to
124 sequence the genomes of 27 non-human primate species from 26 genera of 11 families (table
125 S1). Long reads were self-polished and assembled, and the genome assemblies were further
126 corrected and polished by paired-end short reads sequenced from the same individuals (tables
127 S2-S4). We also used sequencing data generated by high-throughput Chromosome
128 Conformation Capture technology (28) to anchor assembled contigs into chromosomes for
129 four species (Fig. S1 and table S4). The sizes of the newly assembled genomes of the primate
130 species under study ranged from ~2.4 Gbp (*Daubentonia madagascariensis*) to ~3.1 Gbp
131 (*Erythrocebus patas*), which were mostly consistent with the k-mer-based estimations (Fig.
132 S2 and table S5), with a high average contig N50 length of ~15.9 Mbp (table S6). All the
133 genome assemblies yielded BUSCO complete scores >92% (table S6). A method that
134 integrates *de novo* and homology-based strategies was applied to annotate all genomes with
135 protein sequences from human, chimpanzee, gorilla, orangutan and mouse as references for
136 homology-based gene model prediction. Totals of between 20,066 and 21,468 protein-coding
137 genes were predicted in these genome assemblies (table S7). Further, we also identified ~24.2
138 Mb primate-specific highly conserved elements by using whole-genome alignments between
139 all primates and nine other mammals (Fig. S3).

140

141 The Primate Genome Project also generated high quality reference genomes for another 16
142 primate species which were used in the other accompanying papers to reveal hybrid
143 speciation during the rapid radiation of the macaques (29), the homoploid hybrid speciation in
144 the snub-nosed monkey *Rhinopithecus* genus (30), social evolution in the Asian colobines
145 driven by cold adaptation (31), and the evolutionary adaptations of slow lorises (32). All
146 genomic data have been published openly and can be freely accessed in the NCBI Assembly
147 Database under the accession information described in this study.

148

149 **A genomic phylogeny of living primates**

150 We next performed phylogenomic analyses comprising the 27 newly generated genomes,
151 another 22 published primate genomes, one long-read genome from *Nycticebus pygmaeus*
152 reported in an accompanying paper (32), and two close relatives of primates, the Sunda flying
153 lemur (*Galeopterus variegatus*) and the Chinese tree shrew (*Tupaia belangeri chinensis*) (33),
154 as outgroups (table S8). We constructed whole genome-wide phylogenetic trees using ExaML
155 under a GTR+GAMMA model (34). Altogether, ~ 433.5 Mbp gap-free data of syntenic
156 orthologous sequences were retrieved from the whole-genome alignments (table S9), and
157 were used to infer the primate phylogeny, yielding a high-resolution whole-genome
158 nucleotide evidence tree with identical topology to a previous tree derived from 54 nuclear
159 gene regions from 186 living primates (35). This tree has 100% bootstrap support for all
160 evolutionary nodes, with the exception of the node [*(Symphalangus syndactylus, Hoolock*
161 *leuconedys), Hylobates pileatus*] among gibbon genera with 90% bootstrap support (Figs. 1,
162 S4 and S5). The evolution of gibbons has been characterized by their rapid karyotypic
163 changes, and remains controversial in primate phylogeny at the genus level (24, 35, 36). To
164 confirm the phylogeny of this node, we also generated partitioned trees with orthologous
165 protein-coding genes, exon codons with 1st and 2nd positions, four-fold degenerate sites and

166 conserved non-exonic elements (Figs. S6-S9). The tree from conserved non-exonic elements
167 yielded the identical topologies for the gibbon lineages with the whole-genome nucleotide
168 evidence trees (Fig.S9). However, the trees from orthologous protein-coding genes/exon
169 codons with 1st and 2nd positions and four-fold degenerate sites respectively supported the
170 alternative topologies, [((*Nomascus*, *Hylobates*), (*Symphalangus*, *Hoolock*))] and
171 [((*Nomascus*, (*Symphalangus*, *Hoolock*)), *Hylobates*)] (Figs. S6-S8). The two topologies were
172 shown in previous studies based on variants called by mapping short-reads to the reference
173 genome of *Nomascus leucogenys* (24, 36).

174
175 Our analyses again confirmed the phylogenetic challenge within the gibbon lineage which has
176 experienced pronounced adaptive radiation within an extremely short evolutionary time
177 period (24, 35). Consistently, we observed extremely short internal branches in this lineage on
178 the phylogeny. A comparative analysis using CoalHMM (37) across primate lineages showed
179 that the gibbon lineage represents one of the lineages with the highest frequency of
180 incomplete lineage sorting (38), supporting a previous study based on population data (24).
181 Specifically, the two gibbon branches showed incomplete lineage sorting proportions of 57%
182 and 61%, respectively, but the species topology inferred from incomplete lineage sorting
183 analyses is identical to those presented in this paper (Figs. S4 and S10).

184
185 Based on the whole-genome nucleotide evidence tree and fossil calibration data (35, 39)
186 (Figs. 1 and S11), the divergence dating of living primates was estimated by means of the
187 MCMCtree algorithm (40) (Figs. 1 and S12). We estimated that the most recent common
188 ancestor of all primates evolved between 64.95 and 68.29 million years ago (Mya), which is
189 close to the estimate given in the latest phylogenetic study across mammals (41), suggesting
190 the origin of the primate group near the Cretaceous/Tertiary boundary at 65Mya. Meanwhile,
191 we also estimated that the most recent common ancestor of Strepsirrhini appeared between
192 52.57 to 56.56 Mya and that of the Simiiformes emerged between 35.65 to 42.55 Mya (Figs. 1
193 and S12).

194

195 **Genomic structure and evolution of primates**

196 ***Karyotype evolution and genome rearrangement***

197 The speciation process is often accompanied by karyotypic evolution, which would also
198 impact genome evolution and gene function (42-44). We reconstructed the ancestral
199 karyotype evolutionary process across primate lineages (table S10) and observed an overall
200 conserved pattern of chromosome-level synteny (Fig. 2A). The numbers of ancestral
201 karyotypes of Catarrhini ($2n=46$) and Hominoidea ($2n=48$) were consistent with previous
202 inferences derived from the fluorescence in situ hybridization data of bacterial artificial
203 chromosomes (45) (Fig. 2A). However, we deduced that both of the ancestral karyotypes of
204 primates and Simiiformes had a diploid number of $2n=52$ (Fig. 2A), rather than $2n=50$ as
205 previously suggested (45), recovering a fission event in Chromosome 8 which was observed
206 in the common ancestor of primates (Figs. 2A and S13). Fusion and fission are the most
207 common mechanisms of karyotype evolution in primates, as exemplified by the fusion of
208 Chromosome 2 which occurred specifically in the human lineage (45). Our analyses further
209 identified at least one fission and one fusion during the emergence of the Simiiformes, as well

210 as one fission and four fusions associated with the Catarrhini node (Figs. 2B and S13),
211 resulting in the contemporary karyotype structure of our own. The rapid change of karyotypes
212 in the Simiiformes also led to an increased chromosome number in New World monkeys
213 which possess the largest number of chromosomes across primates. We further estimated the
214 rate of genome rearrangement by taking account of all large-scale genomic rearrangement
215 events including reversions, translocations, fusions and fissions in key evolutionary nodes
216 from the primate common ancestral lineage leading to the human lineage. We observed an
217 increasing rate of rearrangement in the Hominae (*Gorilla-Homo-Pan*) (~2.38/Mya) and
218 particularly in the Hominini (*Homo-Pan*) (~5.56/Mya) (Fig. 2B), which contradicts the
219 Hominini slowdown hypothesis on the nucleotide substitution rates (35).

220

221 ***Lineage-specific segmental duplication***

222 We next compiled segmental duplication maps (Segmental duplication length \geq 5kbp) for
223 primates and 5 outgroup species (Fig. S14 and table S11). Compared with other primate
224 lineages, we observed a striking increase in the number of lineage-specific segmental
225 duplications (221 specific segmental duplications) in the great ape genomes (Fig. 3A and
226 table S12), consistent with previous findings describing a burst of segmental duplications in
227 the great ape ancestor (46). These specific segmental duplications in great apes overlapped
228 with 57 protein-coding genes (table S13), 20 of which were highly expressed in the human
229 brain (Fig. S15). Additionally, we also observed lineage-specific segmental duplications in
230 other primate groups producing lineage-specific novel genes that might have contributed to
231 the evolution of these lineages (table S13). We further explored the functions of all genes
232 overlapping segmental duplications in primate genomes (table S13) against the Human Gene
233 Mutation Database (47) and found that a high proportion of these genes (52.8%) have been
234 reported to be associated with inherited conditions including autism, intellectual disability and
235 other developmental disorders (Fig. 3B and table S14).

236

237 ***Evolution of genome size and transposable elements***

238 Compared to other mammalian groups, the primates have a relatively large genome size on
239 average (48, 49). Among primates, the lemurs (Lemuriformes + Chiromyiformes) were found
240 to be characterized by a significantly smaller genome size (~2.36 Gbp) than those of other
241 groups, such as the lorisooids (Lorisiformes: Lorisidae + Galagidae) (~2.70 Gbp), New World
242 monkeys (~2.82 Gbp), Old World monkeys (~2.91 Gbp) and Hominoidea (~2.96 Gbp) ($P <$
243 0.05, Mann-Whitney U test) (Fig. S16). The increase of genome size in the Simiiformes can
244 be attributed to the expansion of transposable elements (Figs. S16-S18 and table S15),
245 especially *Alu* elements, ~300 nucleotide short interspersed sequence elements (SINEs) that
246 make up ~11% of the human genome (50-54). We observed that the genomes of lemurs
247 exhibited a relative paucity of SINEs, especially *Alu* (~3.87%), which is less than one third of
248 the proportion noted in other lineages (Figs. S16-S18). By contrast, the *Alu* elements in both
249 Simiiformes and Lorisiformes experienced major bursts of retrotranspositional activity at
250 ~40-45 and ~34-39 Mya independently (Fig. S19). Specifically, we noticed a dramatic
251 expansion of the *AluS*-related subclasses especially *AluSx* in the Simiiformes, whilst the *AluJ*-
252 related subclasses (especially *AluJb*) were the dominant subclasses of *Alu* in the Lorisiformes
253 (Fig. S20).

254

255 ***Variation in the nucleotide substitution rate***

256 We estimated the overall nucleotide substitution rate in primates to be around 1.1×10^{-3}
257 substitutions per site per million years (Figs. 3C, S21, and table S16), which is much lower
258 than the average rate for mammals ($\sim 2.7 \times 10^{-3}$ substitutions per site per million years) and
259 birds ($\sim 1.9 \times 10^{-3}$ substitutions per site per million years) (55). However, the nucleotide
260 substitution rate exhibited a high degree of heterogeneity between primate lineages,
261 potentially due to differences with respect to life history traits (56-58). The New World
262 monkeys evolved the fastest at $\sim 1.4 \times 10^{-3}$ substitutions per site per million years (Figs. 3C and
263 S21). We confirmed the hominoid ‘slowdown’ (35, 59-61) hypothesis by detecting a reduced
264 substitution rate in hominoids ($\sim 0.8 \times 10^{-3}$ substitutions per site per million years) (Fig. S21).
265 Meanwhile, our analysis and a previous study (62) suggest that tarsiers, as the most basal
266 haplorrhines, potentially evolved with a rapid substitution rate compared to other primates
267 (Fig. S21).

268

269 ***Evolution of protein-coding genes***

270 We obtained a high-confidence orthologous gene set comprising 10,185 orthologs across 50
271 primate species, Sunda flying lemur and Chinese tree shrew. Based on the whole-genome
272 nucleotide evidence tree topology of primates, we calculated d_N/d_S [the ratio of the rates of
273 nonsynonymous (d_N) to synonymous (d_S) substitutions] for each ortholog to explore the
274 evolutionary constraints operating on coding regions. Based upon the observation that tissue-
275 specific expressed genes are generally conserved across diverse species (63, 64), we
276 estimated the evolutionary rate of tissue-specific expressed genes for different tissues across
277 evolutionary clades in primates, and observed that testis- and spleen-specific expressed genes
278 generally display higher values of d_N/d_S (Figs. 3D, S22, and S23) than other tissue-specific
279 expressed genes, corroborating the rapid evolution of the reproductive and immune systems in
280 primates (65, 66). By contrast, brain-specific expressed genes generally showed a high degree
281 of conservation with lower d_N/d_S values as previously reported, despite the rapid evolution of
282 primate cognitive functions (67).

283

284 Next, we detected 82 positively selected genes in the common ancestral lineage of primates
285 by comparison with other mammalian species (table S17) using the codeml algorithm under
286 the branch-site model with a likelihood rate test in PAML4 (40, 68). We found that these
287 positively selected genes were significantly enriched in genes exhibiting high level expression
288 in brain, bone marrow and testis (table S18). In particular, close to 37% (30 genes) of
289 positively selected genes exhibited biased expression in the brain (tables S18 and S19), and we
290 found that some of them, e.g., *SPTAN1*, *MYT1L* and *SHMT1*, should have important roles in
291 brain function, because deleterious mutations of these genes have been reported to cause brain
292 disorders (69-71) such as ‘epilepsy’ and ‘schizophrenia’. These genes may be important
293 candidates for involvement in the evolution of the primate brain because of their functional
294 importance. Our results suggest that some positively selected genes in the primate ancestral
295 lineage may have been involved in the rapid evolution of their brain functions, despite the
296 general conservation of brain-specific expressed genes. In addition, several immune-related
297 genes (e.g., *XRCC6* and *CD2*) (table S17) also experienced positive selection in the primate

298 ancestor, suggesting that the adaptive immune system might also have contributed to primate
299 evolution.

300

301 **An increased level of genomic change in the ancestor of the Simiiformes**

302 To provide new insights into the genetic underpinnings of primate phenotypic evolution, we
303 performed various comparative genomic analyses including identification of positively
304 selected genes, genes having conserved non-coding regions that have been subject to lineage-
305 specific accelerated evolution (72), and expanded gene families in different primate lineages
306 (68). Intriguingly, an increased level of genomic evolutionary changes, reflected by the high
307 numbers of positively selected genes, lineage-specific accelerated regions and expanded gene
308 families, was observed in the Simiiformes ancestor (Fig. 4A). Consistently, the Simiiformes
309 have also experienced rapid evolution of a series of complex traits in contrast to the
310 Strepsirrhini and Tarsiiformes. For example, the Simiiformes generally exhibit a larger brain
311 volume and body mass than the Strepsirrhini and Tarsiiformes (Fig. 4B) (73, 74). Functional
312 enrichment analyses showed that the associated genes relevant to these rapid genomic
313 changes in the Simiiformes ancestor (tables S20-S22) were over-represented in functions
314 related to the nervous system and development, such as postsynaptic density, synapse and the
315 negative regulation of the canonical Wnt signaling pathway (table S23).

316

317 Additional analyses indicated that various candidate genes in the Simiiformes ancestral
318 lineage, comprising 168 positively selected genes, 273 genes associated with lineage-specific
319 accelerated regions, and 14 expanded gene families, were enriched in central nervous system
320 terms, i.e., brain, cerebrum, cerebellum, hippocampus and cerebral cortex (table S24). More
321 specifically, five genes participated in the pathway ‘axon guidance’ (Fig. 4C), being
322 expressed in the human brain at a high level (table S25). Axon guidance represents a key
323 stage in the formation of a neural network (75, 76) and may have been an important influence
324 on brain volume. In this pathway, two semaphorin genes (*SEMA3B* and *SEMA3D*), which are
325 critical for central nervous system patterning (77, 78), experienced positive selection and
326 served as a gene associated with the lineage-specific accelerated region, respectively. These
327 two genes, together with another three genes associated with the lineage-specific accelerated
328 regions (*EPHA3*, *RAC1* and *NTNG2*), are known to be important for brain development (79-
329 81). Furthermore, eight genes were assigned under the term ‘Hippo signaling pathway’ (Fig.
330 4D), an evolutionarily conserved signaling pathway, which controls organ or body size by
331 regulating cell growth, proliferation and apoptosis in a range of animals, from flies to humans
332 (82-84). Taken together, genes involved in neuronal network formation and the control of
333 organ size appear to have undergone adaptive evolution in the Simiiformes ancestral lineage
334 and may have been responsible for specific phenotypic changes, particularly the progressive
335 increase in brain volumes and body sizes as compared with the Tarsiiformes and Strepsirrhini.

336

337 A major phenotypic difference between the Strepsirrhini/Tarsiiformes and the Simiiformes is
338 nocturnal versus diurnal life history. The visual system has diverged substantially between the
339 Simiiformes and Strepsirrhini/Tarsiiformes such that the diurnal Simiiformes have much
340 smaller corneal sizes (relative to their eyes) and higher visual acuity than the
341 Strepsirrhini/Tarsiiformes (85). Consistent with this phenotypic difference, we detected

342 positive selection signals in three genes (*NPHP4*, *GRHL2* and *SLC39A5*) associated with ‘eye
343 development’ (GO: 0001654) in the Simiiformes ancestral lineage. An intragenic deletion in
344 *NPHP4* causes recessive cone-rod dystrophy with a predominant loss of cone function in the
345 dachshund (86). *GRHL2* encodes a transcription factor that suppresses epithelial-to-
346 mesenchymal transition; ectopic *GRHL2* expression due to mutation accelerates cell state
347 transition and leads to posterior polymorphous corneal dystrophy and vision function
348 disruption (87). The *GRHL2* gene has the highest number of positively selected sites in the
349 Simiiformes ancestor compared with the other genes involved in ‘eye development’ (Fig.
350 S24). *TAS1R1* encodes a taste receptor which can form a heterodimer with *TAS1R3* to elicit
351 the umami taste (88). We found that *TAS1R1* also experienced positive selection with four
352 positively selected sites in the Simiiformes ancestor (Fig. 4E). The rapid and concerted
353 evolution of taste receptors and vision could have helped the diurnal Simiiformes to locate
354 and identify food. The detailed functional consequences of these amino acid changes might be
355 worthy of further study.

356

357 Compared to the Strepsirrhini/Tarsiiformes, the Simiiformes generally exhibit darker skin
358 pigmentation and a less bright coat colour (Fig. S25) (89). We identified two pigmentation-
359 related genes (*KIT* and *CREB3L4*) participating in the ‘Melanogenesis’ pathway that evolved
360 under positive selection (detected by the branch-site model) in the Simiiformes ancestor (Fig.
361 4E). Melanocytes play an important role during the formation of skin and coat colors in
362 mammals by regulating melanin-related genes (90). *KIT*, a proto-oncogene, encodes a
363 receptor tyrosine kinase which regulates cell migration, proliferation and differentiation in
364 melanocytes and plays a key role in melanin deposition (91, 92). Additionally, *KIT* also
365 communicates with *MITF*, a key gene in the formation of melanin which regulates the
366 development of melanocytes (93-95).

367

368 **Genetic mechanisms underlying primate phenotype evolution**

369 Primates have evolved diverse phenotypic traits in order to adapt to their challenging
370 environments. Here, we sought to investigate the evolution of complex phenotypes in the
371 brain, skeletal system, body size, digestive system and sense organs in primates.

372

373 ***Brain evolution***

374 In primates, brain volumes range from less than about 2 cm³ in the mouse lemur to
375 approximately 1300 cm³ in human (73). To reveal the genetic changes that might underlie
376 brain evolution in primates, we detected signals of positive selection in brain development
377 genes using a branch-site model in PAML in key evolutionary nodes in the primate
378 phylogeny. A total of 34 brain genes were found to be under positive selection in one of the
379 primate evolutionary nodes (table S26) (68). Four of them (*SLC6A4*, *NR2E1*, *NIPBL*, and
380 *XRCC6*) were under positive selection in the common ancestor of all primates whereas 30
381 were under positive selection in other primate ancestral nodes leading to the evolution of
382 human (table S26). These results appear to suggest that primates underwent continuous brain
383 evolution over an extended period of evolutionary time. Knockout experiments on many of
384 these positively selected genes have shown brain function impairment in mice. For instance,
385 the *NIPBL* gene interacts with *ZFP609* to regulate the migration of cortical neurons, and its

386 mutations are frequently involved in brain neurological defects encompassing intellectual
387 disability and seizures (96). We identified two amino acid residues in the NIPBL protein
388 which experienced adaptive change in the common ancestor of all primates lineage (Fig.
389 S26).

390
391 Microcephaly is characterized by severe neurological defects, the small brain size being
392 caused by disturbance of the proliferation of nerve cells (97). Some genes involved in
393 microcephaly have been proposed as candidates for involvement in the evolution of brain size
394 (98-100). We also searched for positive selection signals in the 1,113 coding genes involved
395 in Microcephaly (HP:0000252). In total, 65 positively selected genes with functional roles in
396 microcephaly were identified along with the primate ancestor leading to the human lineage
397 (table S27), suggesting that microcephaly genes may have been involved in the dramatic
398 evolutionary expansion of brain size that characterizes primates, especially in those crucial
399 evolutionary nodes characterized by a sharp increase in the degree of cortical folding
400 (gyrification) and brain volume (101).

401
402 We next sought to investigate the roles of regulatory elements in the evolution of primate
403 brain size. We first identified non-coding regions that were highly conserved and under strong
404 purifying selection across all primates, and detected signals of accelerated evolution in four
405 lineages [the Simiiformes ancestor (table S21), the Catarrhini ancestor (table S28), the
406 ancestor of great apes (table S29), and the human lineage (table S30)], representing crucial
407 evolutionary nodes for the enlargement of primate brain size (101) (Fig. S27). These lineage-
408 specific accelerated regions should be under strong positive selection specifically in the
409 targeted lineages and might contribute to the adaptation or innovation of these lineages (72).
410 We found 15 genes associated with lineage-specific accelerated regions in the common
411 ancestor of the great apes which showed particularly high expression in the human fetal brain
412 (Fig. S27 and table S31) ($P = 0.023$, Modified Fisher's Exact test); over half of these genes
413 have been reported to have roles in brain development and function (102-109). For example,
414 knockout of the transcription factor-encoding *MEF2C* in a mouse model results in impaired
415 neuronal differentiation and smaller somal size among neural progenitor cells (108).
416 Coincidentally, the lineage-specific accelerated region of this gene was detected in the great
417 ape ancestral lineage. The *DLG5* gene, required for polarization of citron kinase in mitotic
418 neural precursors, also contains a lineage-specific accelerated region in the great ape lineage,
419 and *DLG5*^{-/-} mice have smaller brains and thinner neocortices (109, 110).

420
421 We further investigated the evolution of neurotransmitters, which mediate the neurogenesis
422 process in brain (111, 112) and also play a role in the regulation of brain size (111). We
423 detected 12 positively selected genes and 39 genes associated with lineage-specific
424 accelerated regions in the ancestral nodes leading to the human lineage that were found to be
425 involved in the release, transportation and reception of neurotransmitter signals (Figs. 5A and
426 S28); these genes participate in diverse neurotransmitter systems (i.e., glutamatergic,
427 dopaminergic, cholinergic and GABAergic synapses, and the synaptic vesicle cycle). Among
428 these genes, 5 positively selected genes and 33 genes associated with lineage-specific
429 accelerated regions are highly expressed in human brain (table S32). Taken together, it is

430 likely that at least some of these genomic changes impacting the neurotransmitter signaling
431 pathway might have played a role in primate brain evolution.

432

433 ***Evolution of the skeletal system and limbs***

434 The arboreal lifestyle co-evolved with adaptive changes of the skeletal system and limb
435 development. Here, genes functioning in bone development are likely to have been especially
436 important for the adaptive radiation of the primates. We identified four positively selected
437 genes (*PIEZO1*, *EGFR*, *BMPER* and *NOTCH2*) that were involved in bone development (113-
438 116) in the ancestral lineage of primates (table S17). Bone development requires the
439 recruitment of osteoclast precursors from the surrounding mesenchyme, thereby actuating the
440 key events of bone growth such as marrow cavity formation, capillary invasion and matrix
441 remodelling. Mechanical sensing protein PIEZO1 accommodates bone homeostasis via
442 osteoclast-osteoblast crosstalk (113). Osteoclasts then influence osteoblast formation and
443 differentiation through the secretion of some soluble factors (117). In the meantime, *EGFR*
444 negatively regulates mTOR signaling during osteoblast differentiation to control bone
445 development (114). The *NOTCH2* gene regulates cancellous bone volume and
446 microarchitecture in osteoblast precursors (116, 118).

447

448 Although tails vary across the primates in terms of their length and shape, they generally play
449 key roles in relation to locomotion (119). This notwithstanding, the tail was secondarily lost
450 in some primate lineages including the common ancestor of the apes (120, 121). We retrieved
451 151 genes associated with lineage-specific accelerated regions in the common ancestral
452 lineage of the apes (table S33), including *KIAA1217* (sickle tail protein homolog) (Figs. S29
453 and S30). Mutations in *KIAA1217* are associated with malformations of the notochord and
454 caudal vertebrae in human and affect the development of the vertebral column leading to a
455 characteristic short tail due to a reduced number of caudal vertebrae in mouse (122, 123).
456 Thus, the lineage-specific accelerated region may serve as a regulator of the expression of
457 *KIAA1217* because this lineage-specific accelerated region, residing in the vicinity of
458 *KIAA1217* in the ape lineage, overlaps with an enhancer EH38E1455433 (pELS) (Fig. S31).
459 The high-throughput chromosome conformation capture data (Fig. S32) also showed that this
460 lineage-specific accelerated region is located in the same topologically associated domain as
461 *KIAA1217*, suggesting that they may physically interact with each other (Fig. S32).
462 Furthermore, the lesser apes (gibbons) are of particular interest owing to their dominant
463 locomotor style – brachiation (124, 125). This locomotor adaptation was accompanied by the
464 acquisition of distinct morphological characteristics, particularly the elongated forelimb,
465 representing one of the most intriguing phenotypic traits in gibbons, enabling them to travel
466 through the canopy at high speed (126). We found that positive selection has operated on four
467 genes related to upper limb bone morphology in the gibbon ancestral lineage (table S34). Of
468 these, *NEK1*, which encodes a serine/threonine kinase, contains the most positively selected
469 sites (Fig. 5B). Functional studies have shown that genetic variants in this gene can influence
470 bone length and shorten the humerus and femur in humans (127, 128). Therefore, positive
471 selection acting on genes related to upper limb bone morphology may have been important in
472 the acquisition of the elongated forelimb, a key adaptive trait for the unique brachiating
473 locomotion style of gibbons.

474

475 ***Evolution of body size in primates***

476 Like other mammalian groups (129, 130), extant primate species exhibit a large body size
477 range, from dwarf galagos and mouse lemurs (~60-70g) at one end of the spectrum to male
478 gorillas (>200kg in some individuals) at the other (131). Thus, primate body size has
479 experienced significant divergence, particularly for the great apes with their dramatic
480 enlargement in body size. We detected several positively selected genes in the common
481 ancestors of the great apes which might have contributed to the evolution of this trait. *DUOX2*
482 encodes a protein involved in a critical step of thyroid hormone synthesis and mutations in
483 *DUOX2* are known to cause decreased body size in mouse and panda (132, 133). This gene
484 experienced strong positive selection in the great ape ancestral lineage (χ^2 test, $P = 0.018$)
485 (Fig. 5C and table S35). Additionally, we noted several genes involved in the TGF-beta
486 signaling pathway (e.g., *LTBP1*) or the Wnt signaling pathway (e.g., *MBD2*, *YAP1* and
487 *DISC1*), two of the best known pathways participating in bone development and body size
488 (48), that were either under strong positive selection in the great apes or which have lineage-
489 specific accelerated regions in this lineage (Fig. 5C and tables S29 and S35).

490

491 Several positively selected genes and genes associated with lineage-specific accelerated
492 regions in the great ape ancestor were also significantly overrepresented in the Hippo
493 signaling pathway ($P=0.045$, Modified Fisher's Exact test) (table S36), which has been
494 implicated in the determination of organ and body size (82). Interestingly, when combining
495 all positively selected genes, genes associated with lineage-specific accelerated regions, and
496 expanded gene families in the Simiiformes ancestral lineage, which dramatically increased
497 their body size compared with non-Simiiformes lineages (Fig. 4B), we also detected diverse
498 candidate genes with adaptive changes in the Hippo signaling pathway. These results indicate
499 potentially important roles for the Hippo pathway in body size changes in these two nodes
500 during primate evolution.

501

502 ***Evolution of the digestive system***

503 Primate lineages have evolved diverse dietary habits and specialized digestive functions
504 (134). In particular, leaf-eating Colobines, an African and Asian subfamily (Colobinae) of
505 Old World monkeys, have evolved a uniquely specialized and compartmentalized foregut,
506 with discrete alkaline and acidic sections (to cope with their folivorous diet), in which
507 microbial fermentation can take place (135, 136). Although colobines eat leaves, fruits,
508 flowers and seeds, they typically focus much of their feeding time on leaves [estimated range:
509 ~34-81% of their annual diet] (135). Accordingly, these leaf-eaters are well adapted in terms
510 of meeting their energy metabolism requirements, balancing micronutrients and protein
511 intake, while also dealing with the toxins contained in their food plants (137).

512

513 In the ancestor of the Colobinae, we identified a number of pivotal digestive genes that
514 underwent positive selection (table S37). Acyl-CoA dehydrogenase, encoded by the *ACADM*
515 gene, is an important lipolytic enzyme which catalyzes the initial step in each cycle of
516 mitochondrial fatty acid β -oxidation and plays a key role in metabolizing fatty acids derived
517 from ingested foods (138). Energy-rich short-chain volatile fatty acids are produced by the

518 microbial fermentation process; these are absorbed by the host and make an important
519 contribution to the energy budget of colobines (135). Therefore, rapid evolution of this gene,
520 with two positively selected sites (V75M and A138C), may have been important for the
521 absorption of fatty acids by Colobines (Fig. 5D and S33). *NOX1*, which is highly expressed
522 in the colon, was identified as being under positive selection in the ancestor of the Colobinae
523 (Fig. 5D and tables S37 and S38). *NOX1*-dependent ROS production can further regulate
524 microorganism homeostasis in the ileum of mice (139). The rumens of ruminants and the
525 saccus stomachs of Colobines, have developed a similar adaptive strategy to allow the
526 microbial fermentation of high fibre foods, and hence are an example of convergent
527 evolution. We found that *MYBPCI*, which has been shown to contribute to morphological and
528 functional differences in the bovine rumen (140), also underwent positive selection in the
529 ancestor of the Colobinae (Fig. 5D and table S37). In addition, 100 genes associated with
530 lineage-specific accelerated regions were identified in the ancestral lineage of the Colobinae
531 (table S39). Several of these genes were also highly expressed in the stomach, colon, pancreas
532 and small intestine (Fig. 5D and table S38). Of these, *RNASE4* encodes a vital digestive
533 enzyme, pancreatic ribonuclease 4, and is a paralog of *RNASE1* which is known to have
534 undergone adaptive evolution by gene duplication in leaf-eating Colobines and howler
535 monkeys (26, 141). Colobines may therefore have acquired adaptations to allow them to
536 digest fatty acids and ribonucleic acids, whilst their unique foregut and intestinal microbiota
537 enabled them to cope with their folivorous diet.

538

539 ***Evolution of sensory organs***

540 In many mammals, olfaction is the dominant sense and provides much of the sensory
541 information upon which animals rely to navigate, forage and avoid predators, or for social
542 behaviour and courtship (134). Most Strepsirrhini species are nocturnal, whereas most
543 Simiiformes are diurnal with well-developed colour vision systems attuned to their priorities
544 in diurnal activity (142-145). By contrast, olfactory sensitivity would appear to have
545 decreased in the Simiiformes as compared to the Strepsirrhini (134, 146, 147). Consistent
546 with these findings, we found that the copy number of several specific olfactory receptor gene
547 families was significantly reduced in the Simiiformes. For example, the olfactory receptor
548 gene family, *OR52A*, underwent the significant contraction in the Simiiformes (40 species)
549 with only ~0.7 copies on average, in contrast to ~3.4 average copies in the Strepsirrhini (nine
550 species) (Figs. S34 and S35) ($P = 4.072e-05$, Mann-Whitney U test). Anatomically,
551 Strepsirrhini are characterized by the presence of a rhinarium, a moist and naked surface
552 around the tip of the nose which is present in most mammals including dogs and cats, but the
553 rhinarium has been lost in the Simiiformes (134, 147). Olfactory bulb volume, which
554 correlates with olfactory receptor neuron population size, is also larger in the Strepsirrhini
555 than in the Simiiformes (146, 148). Intriguingly, the *LHX2* gene, which participates in
556 olfactory bulb development (149, 150), experienced positive selection in the ancestor of the
557 Strepsirrhini ($P = 0.03$, χ^2 test, table S40).

558

559 **Demographic history of non-human primates**

560 The IUCN lists more than a third of primates as being critically endangered or vulnerable (1).
561 To evaluate the effects of climate change and human activity on their recent population

562 declines, we inferred their demographic histories over the past million years by using the
563 pairwise sequentially Markovian coalescent model (PSMC) (151) for each primate species in
564 this study (Fig. S36 and tables S16 and S41). Our data showed that most non-human primate
565 species have experienced rapid population declines during the late Pleistocene (Figs. 6A and
566 S37), consistent with the record of large mammal mass extinction in this period (48, 152).
567 Although we did not observe a significant difference between endangered species and other
568 species in terms of nucleotide diversity (Fig. S38 and table S42), we did detect a significant
569 positive correlation between the median effective population size (N_e) over the past ~20,000
570 years and nucleotide diversity ($P = 0.002$, Pearson's product-moment correlation, after
571 phylogenetic correction) (Fig. 6B and table S42), indicating a long-term effect of N_e decline
572 on the loss of genetic diversity. According to the historical demographic patterns, we further
573 clustered all non-human primate species with similar trends of historical N_e and found that 20
574 species have experienced a continual N_e decline over the last 3 million years (My) (Fig. 6C).
575 Of note, 65% of these species are now listed as being endangered or critically endangered
576 (Figs. 6C and S39). This ratio is twice that of the remaining species suggesting that the
577 prehistoric environmental effects (e.g., habitat fragmentation) (26) may also have driven
578 population decline and contributed to the current endangered status of these species well
579 before human interference in the modern era.

580

581 **Conclusions**

582 Understanding the evolution and genetic basis of human-specific traits requires a systematic
583 comparison of genomes along the primate lineages. Previous studies of primate genomes have
584 focused on genomic changes in the human lineage that influenced human brain functions and
585 other traits (120, 153-155). Our comparative phylogenomic analyses across primate lineages
586 have revealed some of the accumulated genomic changes at different primate ancestral nodes
587 that may have contributed to the evolution of uniquely human traits. Of particular interest, we
588 report a hitherto unreported increase in the rate of genomic change in the Simiiformes
589 common ancestor that may have played a role in the later diversification of Simiiformes and
590 the evolution of humans. Our comparative genomic analyses also yielded insights into the
591 genetic basis of phenotypic diversity across primate lineages. With the rich diversity of
592 morphology and physiology among non-human primates, further genomic analyses covering
593 all primate species promise to provide an indispensable resource for comparative studies
594 allowing expansion of the scope of biomedical research programs using primates as model
595 systems. Further, increased knowledge of the genomic makeup and variations of non-human
596 primates should help to identify risk factors for genetic disorders and enhance wildlife health
597 management in both wild and captive members of these species.

598

599 **References and Notes**

- 600 1. A. Estrada, P. A. Garber, A. B. Rylands, C. Roos, E. Fernandez-Duque, A. Di Fiore,
601 K. A. Nekaris, V. Nijman, E. W. Heymann, J. E. Lambert, F. Rovero, C. Barelli, J.
602 M. Setchell, T. R. Gillespie, R. A. Mittermeier, L. V. Arregoitia, M. de Guinea, S.
603 Gouveia, R. Dobrovolski, S. Shanee, N. Shanee, S. A. Boyle, A. Fuentes, K. C.
604 MacKinnon, K. R. Amato, A. L. Meyer, S. Wich, R. W. Sussman, R. Pan, I. Kone, B.

- 605 Li, Impending extinction crisis of the world's primates: why primates matter. *Sci Adv*
606 **3**, e1600946 (2017).
- 607 2. C. Roos, K. M. Helgen, R. P. Miguez, N. M. L. Thant, N. Lwin, A. K. Lin, A. Lin, K.
608 M. Yi, P. Soe, Z. M. Hein, M. N. N. Myint, T. Ahmed, D. Chetry, M. Urh, E. G.
609 Veatch, N. Duncan, P. Kamminga, M. A. H. Chua, L. Yao, C. Matauschek, D. Meyer,
610 Z. J. Liu, M. Li, T. Nadler, P. F. Fan, L. K. Quyet, M. Hofreiter, D. Zinner, F.
611 Momberg, Mitogenomic phylogeny of the Asian colobine genus *Trachypithecus* with
612 special focus on *Trachypithecus phayrei* (Blyth, 1847) and description of a new
613 species. *Zool Res* **41**, 656-669 (2020).
- 614 3. A. Nater, M. P. Mattle-Greminger, A. Nurcahyo, M. G. Nowak, M. de Manuel, T.
615 Desai, C. Groves, M. Pybus, T. B. Sonay, C. Roos, A. R. Lameira, S. A. Wich, J.
616 Askew, M. Davila-Ross, G. Fredriksson, G. de Valles, F. Casals, J. Prado-Martinez,
617 B. Goossens, E. J. Verschoor, K. S. Warren, I. Singleton, D. A. Marques, J.
618 Pamungkas, D. Perwitasari-Farajallah, P. Rianti, A. Tuuga, I. G. Gut, M. Gut, P.
619 Orozco-terWengel, C. P. van Schaik, J. Bertranpetit, M. Anisimova, A. Scally, T.
620 Marques-Bonet, E. Meijaard, M. Krützen, Morphometric, behavioral, and genomic
621 evidence for a new orangutan species. *Curr Biol* **27**, 3487-3498 (2017).
- 622 4. P. F. Fan, K. He, X. Chen, A. Ortiz, B. Zhang, C. Zhao, Y. Q. Li, H. B. Zhang, C.
623 Kimock, W. Z. Wang, C. Groves, S. T. Turvey, C. Roos, K. M. Helgen, X. L. Jiang,
624 Description of a new species of *Hoolock* gibbon (Primates: Hylobatidae) based on
625 integrative taxonomy. *Am J Primatol* **79**, e22631 (2017).
- 626 5. C. Li, C. Zhao, P. F. Fan, White-cheeked macaque (*Macaca leucogenys*): a new
627 macaque species from Medog, southeastern Tibet. *Am J Primatol* **77**, 753-766 (2015).
- 628 6. J. Rogers, R. A. Gibbs, Comparative primate genomics: emerging patterns of genome
629 content and dynamics. *Nat Rev Genet* **15**, 347-359 (2014).
- 630 7. B. Rockx, T. Kuiken, S. Herfst, T. Bestebroer, M. M. Lamers, B. B. Oude Munnink,
631 D. de Meulder, G. van Amerongen, J. van den Brand, N. M. A. Okba, D. Schipper, P.
632 van Run, L. Leijten, R. Sikkema, E. Verschoor, B. Verstrepen, W. Bogers, J.
633 Langermans, C. Drost, M. Fentener van Vlissingen, R. Fouchier, R. de Swart, M.
634 Koopmans, B. L. Haagmans, Comparative pathogenesis of COVID-19, MERS, and
635 SARS in a nonhuman primate model. *Science* **368**, 1012-1015 (2020).
- 636 8. A. Chandrashekar, J. Liu, A. J. Martinot, K. McMahan, N. B. Mercado, L. Peter, L.
637 H. Tostanoski, J. Yu, Z. Maliga, M. Nekorchuk, K. Busman-Sahay, M. Terry, L. M.
638 Wrijil, S. Ducat, D. R. Martinez, C. Atyeo, S. Fischinger, J. S. Burke, M. D. Slein, L.
639 Pessaint, A. Van Ry, J. Greenhouse, T. Taylor, K. Blade, A. Cook, B. Finneyfrock, R.
640 Brown, E. Teow, J. Velasco, R. Zahn, F. Wegmann, P. Abbink, E. A. Bondzie, G.
641 Dagotto, M. S. Gebre, X. He, C. Jacob-Dolan, N. Kordana, Z. Li, M. A. Lifton, S. H.
642 Mahrokhian, L. F. Maxfield, R. Nityanandam, J. P. Nkolola, A. G. Schmidt, A. D.
643 Miller, R. S. Baric, G. Alter, P. K. Sorger, J. D. Estes, H. Andersen, M. G. Lewis, D.
644 H. Barouch, SARS-CoV-2 infection protects against rechallenge in rhesus macaques.
645 *Science* **369**, 812-817 (2020).
- 646 9. Q. Gao, L. Bao, H. Mao, L. Wang, K. Xu, M. Yang, Y. Li, L. Zhu, N. Wang, Z. Lv,
647 H. Gao, X. Ge, B. Kan, Y. Hu, J. Liu, F. Cai, D. Jiang, Y. Yin, C. Qin, J. Li, X. Gong,
648 X. Lou, W. Shi, D. Wu, H. Zhang, L. Zhu, W. Deng, Y. Li, J. Lu, C. Li, X. Wang, W.

- 649 Yin, Y. Zhang, C. Qin, Development of an inactivated vaccine candidate for SARS-
650 CoV-2. *Science* **369**, 77-81 (2020).
- 651 10. J. Yu, L. H. Tostanoski, L. Peter, N. B. Mercado, K. McMahan, S. H. Mahrokhian, J.
652 P. Nkolola, J. Liu, Z. Li, A. Chandrashekar, D. R. Martinez, C. Loos, C. Atyeo, S.
653 Fischinger, J. S. Burke, M. D. Slein, Y. Chen, A. Zuiani, F. J. N. Lelis, M. Travers, S.
654 Habibi, L. Pessaint, A. Van Ry, K. Blade, R. Brown, A. Cook, B. Finneyfrock, A.
655 Dodson, E. Teow, J. Velasco, R. Zahn, F. Wegmann, E. A. Bondzie, G. Dagotto, M.
656 S. Gebre, X. He, C. Jacob-Dolan, M. Kirilova, N. Kordana, Z. Lin, L. F. Maxfield, F.
657 Nampanya, R. Nityanandam, J. D. Ventura, H. Wan, Y. Cai, B. Chen, A. G. Schmidt,
658 D. R. Wesemann, R. S. Baric, G. Alter, H. Andersen, M. G. Lewis, D. H. Barouch,
659 DNA vaccine protection against SARS-CoV-2 in rhesus macaques. *Science* **369**, 806-
660 811 (2020).
- 661 11. V. J. Munster, F. Feldmann, B. N. Williamson, N. van Doremalen, L. Pérez-Pérez, J.
662 Schulz, K. Meade-White, A. Okumura, J. Callison, B. Brumbaugh, V. A. Avanzato,
663 R. Rosenke, P. W. Hanley, G. Saturday, D. Scott, E. R. Fischer, E. de Wit,
664 Respiratory disease in rhesus macaques inoculated with SARS-CoV-2. *Nature* **585**,
665 268-272 (2020).
- 666 12. N. B. Mercado, R. Zahn, F. Wegmann, C. Loos, A. Chandrashekar, J. Yu, J. Liu, L.
667 Peter, K. McMahan, L. H. Tostanoski, X. He, D. R. Martinez, L. Rutten, R. Bos, D.
668 van Manen, J. Vellinga, J. Custers, J. P. Langedijk, T. Kwaks, M. J. G. Bakkers, D.
669 Zuijdggeest, S. K. Rosendahl Huber, C. Atyeo, S. Fischinger, J. S. Burke, J. Feldman,
670 B. M. Hauser, T. M. Caradonna, E. A. Bondzie, G. Dagotto, M. S. Gebre, E.
671 Hoffman, C. Jacob-Dolan, M. Kirilova, Z. Li, Z. Lin, S. H. Mahrokhian, L. F.
672 Maxfield, F. Nampanya, R. Nityanandam, J. P. Nkolola, S. Patel, J. D. Ventura, K.
673 Verrington, H. Wan, L. Pessaint, A. Van Ry, K. Blade, A. Strasbaugh, M. Cabus, R.
674 Brown, A. Cook, S. Zouantchangadou, E. Teow, H. Andersen, M. G. Lewis, Y. Cai,
675 B. Chen, A. G. Schmidt, R. K. Reeves, R. S. Baric, D. A. Lauffenburger, G. Alter, P.
676 Stoffels, M. Mammen, J. Van Hoof, H. Schuitemaker, D. H. Barouch, Single-shot
677 Ad26 vaccine protects against SARS-CoV-2 in rhesus macaques. *Nature* **586**, 583-
678 588 (2020).
- 679 13. K. S. Corbett, B. Flynn, K. E. Foulds, J. R. Francica, S. Boyoglu-Barnum, A. P.
680 Werner, B. Flach, S. O'Connell, K. W. Bock, M. Minai, B. M. Nagata, H. Andersen,
681 D. R. Martinez, A. T. Noe, N. Douek, M. M. Donaldson, N. N. Nji, G. S. Alvarado,
682 D. K. Edwards, D. R. Flebbe, E. Lamb, N. A. Doria-Rose, B. C. Lin, M. K. Louder,
683 S. O'Dell, S. D. Schmidt, E. Phung, L. A. Chang, C. Yap, J. M. Todd, L. Pessaint, A.
684 Van Ry, S. Browne, J. Greenhouse, T. Putman-Taylor, A. Strasbaugh, T. A.
685 Campbell, A. Cook, A. Dodson, K. Steingrebe, W. Shi, Y. Zhang, O. M. Abiona, L.
686 Wang, A. Pegu, E. S. Yang, K. Leung, T. Zhou, I. T. Teng, A. Widge, I. Gordon, L.
687 Novik, R. A. Gillespie, R. J. Loomis, J. I. Moliva, G. Stewart-Jones, S. Himansu, W.
688 P. Kong, M. C. Nason, K. M. Morabito, T. J. Ruckwardt, J. E. Ledgerwood, M. R.
689 Gaudinski, P. D. Kwong, J. R. Mascola, A. Carfi, M. G. Lewis, R. S. Baric, A.
690 McDermott, I. N. Moore, N. J. Sullivan, M. Roederer, R. A. Seder, B. S. Graham,
691 Evaluation of the mRNA-1273 Vaccine against SARS-CoV-2 in nonhuman primates.
692 *N Engl J Med* **383**, 1544-1555 (2020).

- 693 14. N. van Doremalen, T. Lambe, A. Spencer, S. Belij-Rammerstorfer, J. N.
694 Purushotham, J. R. Port, V. A. Avanzato, T. Bushmaker, A. Flaxman, M.
695 Ulaszewska, F. Feldmann, E. R. Allen, H. Sharpe, J. Schulz, M. Holbrook, A.
696 Okumura, K. Meade-White, L. Pérez-Pérez, N. J. Edwards, D. Wright, C. Bissett, C.
697 Gilbride, B. N. Williamson, R. Rosenke, D. Long, A. Ishwarbhai, R. Kailath, L. Rose,
698 S. Morris, C. Powers, J. Lovaglio, P. W. Hanley, D. Scott, G. Saturday, E. de Wit, S.
699 C. Gilbert, V. J. Munster, ChAdOx1 nCoV-19 vaccine prevents SARS-CoV-2
700 pneumonia in rhesus macaques. *Nature* **586**, 578-582 (2020).
- 701 15. B. N. Williamson, F. Feldmann, B. Schwarz, K. Meade-White, D. P. Porter, J.
702 Schulz, N. van Doremalen, I. Leighton, C. K. Yinda, L. Pérez-Pérez, A. Okumura, J.
703 Lovaglio, P. W. Hanley, G. Saturday, C. M. Bosio, S. Anzick, K. Barbian, T. Cihlar,
704 C. Martens, D. P. Scott, V. J. Munster, E. de Wit, Clinical benefit of remdesivir in
705 rhesus macaques infected with SARS-CoV-2. *Nature* **585**, 273-276 (2020).
- 706 16. T. Z. Song, H. Y. Zheng, J. B. Han, L. Jin, X. Yang, F. L. Liu, R. H. Luo, R. R. Tian,
707 H. R. Cai, X. L. Feng, C. Liu, M. H. Li, Y. T. Zheng, Delayed severe cytokine storm
708 and immune cell infiltration in SARS-CoV-2-infected aged Chinese rhesus macaques.
709 *Zool Res* **41**, 503-516 (2020).
- 710 17. W. Enard, S. Pääbo, Comparative primate genomics. *Annu Rev Genomics Hum Genet*
711 **5**, 351-378 (2004).
- 712 18. Z. N. Kronenberg, I. T. Fiddes, D. Gordon, S. Murali, S. Cantsilieris, O. S. Meyerson,
713 J. G. Underwood, B. J. Nelson, M. J. P. Chaisson, M. L. Dougherty, K. M. Munson,
714 A. R. Hastie, M. Diekhans, F. Hormozdiari, N. Lorusso, K. Hoekzema, R. Qiu, K.
715 Clark, A. Raja, A. E. Welch, M. Sorensen, C. Baker, R. S. Fulton, J. Armstrong, T. A.
716 Graves-Lindsay, A. M. Denli, E. R. Hoppe, P. Hsieh, C. M. Hill, A. W. C. Pang, J.
717 Lee, E. T. Lam, S. K. Dutcher, F. H. Gage, W. C. Warren, J. Shendure, D. Haussler,
718 V. A. Schneider, H. Cao, M. Ventura, R. K. Wilson, B. Paten, A. Pollen, E. E.
719 Eichler, High-resolution comparative analysis of great ape genomes. *Science* **360**,
720 eaar6343 (2018).
- 721 19. C. S. a. A. Consortium, Initial sequence of the chimpanzee genome and comparison
722 with the human genome. *Nature* **437**, 69-87 (2005).
- 723 20. R. A. Gibbs, J. Rogers, M. G. Katze, R. Bumgarner, G. M. Weinstock, E. R. Mardis,
724 K. A. Remington, R. L. Strausberg, J. C. Venter, R. K. Wilson, M. A. Batzer, C. D.
725 Bustamante, E. E. Eichler, M. W. Hahn, R. C. Hardison, K. D. Makova, W. Miller, A.
726 Milosavljevic, R. E. Palermo, A. Siepel, J. M. Sikela, T. Attaway, S. Bell, K. E.
727 Bernard, C. J. Buhay, M. N. Chandrabose, M. Dao, C. Davis, K. D. Delehaunty, Y.
728 Ding, H. H. Dinh, S. Dugan-Rocha, L. A. Fulton, R. A. Gabisi, T. T. Garner, J.
729 Godfrey, A. C. Hawes, J. Hernandez, S. Hines, M. Holder, J. Hume, S. N. Jhangiani,
730 V. Joshi, Z. M. Khan, E. F. Kirkness, A. Cree, R. G. Fowler, S. Lee, L. R. Lewis, Z.
731 Li, Y. S. Liu, S. M. Moore, D. Muzny, L. V. Nazareth, D. N. Ngo, G. O. Okwuonu,
732 G. Pai, D. Parker, H. A. Paul, C. Pfannkoch, C. S. Pohl, Y. H. Rogers, S. J. Ruiz, A.
733 Sabo, J. Santibanez, B. W. Schneider, S. M. Smith, E. Sodergren, A. F. Svatek, T. R.
734 Utterback, S. Vattathil, W. Warren, C. S. White, A. T. Chinwalla, Y. Feng, A. L.
735 Halpern, L. W. Hillier, X. Huang, P. Minx, J. O. Nelson, K. H. Pepin, X. Qin, G. G.
736 Sutton, E. Venter, B. P. Walenz, J. W. Wallis, K. C. Worley, S. P. Yang, S. M. Jones,

737 M. A. Marra, M. Rocchi, J. E. Schein, R. Baertsch, L. Clarke, M. Csürös, J.
738 Glasscock, R. A. Harris, P. Havlak, A. R. Jackson, H. Jiang, Y. Liu, D. N. Messina,
739 Y. Shen, H. X. Song, T. Wylie, L. Zhang, E. Birney, K. Han, M. K. Konkel, J. Lee,
740 A. F. Smit, B. Ullmer, H. Wang, J. Xing, R. Burhans, Z. Cheng, J. E. Karro, J. Ma, B.
741 Raney, X. She, M. J. Cox, J. P. Demuth, L. J. Dumas, S. G. Han, J. Hopkins, A.
742 Karimpour-Fard, Y. H. Kim, J. R. Pollack, T. Vinar, C. Addo-Quaye, J. Degenhardt,
743 A. Denby, M. J. Hubisz, A. Indap, C. Kosiol, B. T. Lahn, H. A. Lawson, A. Marklein,
744 R. Nielsen, E. J. Vallender, A. G. Clark, B. Ferguson, R. D. Hernandez, K. Hirani, H.
745 Kehrer-Sawatzki, J. Kolb, S. Patil, L. L. Pu, Y. Ren, D. G. Smith, D. A. Wheeler, I.
746 Schenck, E. V. Ball, R. Chen, D. N. Cooper, B. Giardine, F. Hsu, W. J. Kent, A.
747 Lesk, D. L. Nelson, E. O'Brien W, K. Prüfer, P. D. Stenson, J. C. Wallace, H. Ke, X.
748 M. Liu, P. Wang, A. P. Xiang, F. Yang, G. P. Barber, D. Haussler, D. Karolchik, A.
749 D. Kern, R. M. Kuhn, K. E. Smith, A. S. Zwiig, Evolutionary and biomedical
750 insights from the rhesus macaque genome. *Science* **316**, 222-234 (2007).

751 21. A. Scally, J. Y. Duthiel, L. W. Hillier, G. E. Jordan, I. Goodhead, J. Herrero, A.
752 Hobolth, T. Lappalainen, T. Mailund, T. Marques-Bonet, S. McCarthy, S. H.
753 Montgomery, P. C. Schwalie, Y. A. Tang, M. C. Ward, Y. Xue, B. Yngvadottir, C.
754 Alkan, L. N. Andersen, Q. Ayub, E. V. Ball, K. Beal, B. J. Bradley, Y. Chen, C. M.
755 Clee, S. Fitzgerald, T. A. Graves, Y. Gu, P. Heath, A. Heger, E. Karakoc, A. Kolb-
756 Kokocinski, G. K. Laird, G. Lunter, S. Meader, M. Mort, J. C. Mullikin, K. Munch,
757 T. D. O'Connor, A. D. Phillips, J. Prado-Martinez, A. S. Rogers, S. Sajjadian, D.
758 Schmidt, K. Shaw, J. T. Simpson, P. D. Stenson, D. J. Turner, L. Vigilant, A. J.
759 Vilella, W. Whitener, B. Zhu, D. N. Cooper, P. de Jong, E. T. Dermitzakis, E. E.
760 Eichler, P. Flicek, N. Goldman, N. I. Mundy, Z. Ning, D. T. Odom, C. P. Ponting, M.
761 A. Quail, O. A. Ryder, S. M. Searle, W. C. Warren, R. K. Wilson, M. H. Schierup, J.
762 Rogers, C. Tyler-Smith, R. Durbin, Insights into hominid evolution from the gorilla
763 genome sequence. *Nature* **483**, 169-175 (2012).

764 22. M. G. S. a. A. Consortium, The common marmoset genome provides insight into
765 primate biology and evolution. *Nat Genet* **46**, 850-857 (2014).

766 23. D. P. Locke, L. W. Hillier, W. C. Warren, K. C. Worley, L. V. Nazareth, D. M.
767 Muzny, S. P. Yang, Z. Wang, A. T. Chinwalla, P. Minx, M. Mitreva, L. Cook, K. D.
768 Delehaunty, C. Fronick, H. Schmidt, L. A. Fulton, R. S. Fulton, J. O. Nelson, V.
769 Magrini, C. Pohl, T. A. Graves, C. Markovic, A. Cree, H. H. Dinh, J. Hume, C. L.
770 Kovar, G. R. Fowler, G. Lunter, S. Meader, A. Heger, C. P. Ponting, T. Marques-
771 Bonet, C. Alkan, L. Chen, Z. Cheng, J. M. Kidd, E. E. Eichler, S. White, S. Searle, A.
772 J. Vilella, Y. Chen, P. Flicek, J. Ma, B. Raney, B. Suh, R. Burhans, J. Herrero, D.
773 Haussler, R. Faria, O. Fernando, F. Darré, D. Farré, E. Gazave, M. Oliva, A. Navarro,
774 R. Roberto, O. Capozzi, N. Archidiacono, G. Della Valle, S. Purgato, M. Rocchi, M.
775 K. Konkel, J. A. Walker, B. Ullmer, M. A. Batzer, A. F. Smit, R. Hubley, C. Casola,
776 D. R. Schrider, M. W. Hahn, V. Quesada, X. S. Puente, G. R. Ordoñez, C. López-
777 Otín, T. Vinar, B. Brejova, A. Ratan, R. S. Harris, W. Miller, C. Kosiol, H. A.
778 Lawson, V. Taliwal, A. L. Martins, A. Siepel, A. Roychoudhury, X. Ma, J.
779 Degenhardt, C. D. Bustamante, R. N. Gutenkunst, T. Mailund, J. Y. Duthiel, A.
780 Hobolth, M. H. Schierup, O. A. Ryder, Y. Yoshinaga, P. J. de Jong, G. M.

- 781 Weinstock, J. Rogers, E. R. Mardis, R. A. Gibbs, R. K. Wilson, Comparative and
782 demographic analysis of orangutan genomes. *Nature* **469**, 529-533 (2011).
- 783 24. L. Carbone, R. A. Harris, S. Gnerre, K. R. Veeramah, B. Lorente-Galdos, J.
784 Huddleston, T. J. Meyer, J. Herrero, C. Roos, B. Aken, F. Anaclerio, N.
785 Archidiacono, C. Baker, D. Barrell, M. A. Batzer, K. Beal, A. Blancher, C. L.
786 Bohrson, M. Brameier, M. S. Campbell, O. Capozzi, C. Casola, G. Chiatante, A.
787 Cree, A. Damert, P. J. de Jong, L. Dumas, M. Fernandez-Callejo, P. Flicek, N. V.
788 Fuchs, I. Gut, M. Gut, M. W. Hahn, J. Hernandez-Rodriguez, L. W. Hillier, R.
789 Hubley, B. Ianc, Z. Izsvák, N. G. Jablonski, L. M. Johnstone, A. Karimpour-Fard, M.
790 K. Konkel, D. Kostka, N. H. Lazar, S. L. Lee, L. R. Lewis, Y. Liu, D. P. Locke, S.
791 Mallick, F. L. Mendez, M. Muffato, L. V. Nazareth, K. A. Nevenon, M. O'Bleness, C.
792 Ochis, D. T. Odom, K. S. Pollard, J. Quilez, D. Reich, M. Rocchi, G. G. Schumann,
793 S. Searle, J. M. Sikela, G. Skollar, A. Smit, K. Sonmez, B. ten Hallers, E. Terhune, G.
794 W. Thomas, B. Ullmer, M. Ventura, J. A. Walker, J. D. Wall, L. Walter, M. C. Ward,
795 S. J. Wheelan, C. W. Whelan, S. White, L. J. Wilhelm, A. E. Woerner, M. Yandell,
796 B. Zhu, M. F. Hammer, T. Marques-Bonet, E. E. Eichler, L. Fulton, C. Fronick, D.
797 M. Muzny, W. C. Warren, K. C. Worley, J. Rogers, R. K. Wilson, R. A. Gibbs,
798 Gibbon genome and the fast karyotype evolution of small apes. *Nature* **513**, 195-201
799 (2014).
- 800 25. L. Yu, G. D. Wang, J. Ruan, Y. B. Chen, C. P. Yang, X. Cao, H. Wu, Y. H. Liu, Z. L.
801 Du, X. P. Wang, J. Yang, S. C. Cheng, L. Zhong, L. Wang, X. Wang, J. Y. Hu, L.
802 Fang, B. Bai, K. L. Wang, N. Yuan, S. F. Wu, B. G. Li, J. G. Zhang, Y. Q. Yang, C.
803 L. Zhang, Y. C. Long, H. S. Li, J. Y. Yang, D. M. Irwin, O. A. Ryder, Y. Li, C. I.
804 Wu, Y. P. Zhang, Genomic analysis of snub-nosed monkeys (*Rhinopithecus*)
805 identifies genes and processes related to high-altitude adaptation. *Nat Genet* **48**, 947-
806 952 (2016).
- 807 26. X. Zhou, B. Wang, Q. Pan, J. Zhang, S. Kumar, X. Sun, Z. Liu, H. Pan, Y. Lin, G.
808 Liu, W. Zhan, M. Li, B. Ren, X. Ma, H. Ruan, C. Cheng, D. Wang, F. Shi, Y. Hui, Y.
809 Tao, C. Zhang, P. Zhu, Z. Xiang, W. Jiang, J. Chang, H. Wang, Z. Cao, Z. Jiang, B.
810 Li, G. Yang, C. Roos, P. A. Garber, M. W. Bruford, R. Li, M. Li, Whole-genome
811 sequencing of the snub-nosed monkey provides insights into folivory and
812 evolutionary history. *Nat Genet* **46**, 1303-1310 (2014).
- 813 27. A. O. Ayoola, B. L. Zhang, R. P. Meisel, L. M. Nneji, Y. Shao, O. B. Morenikeji, A.
814 C. Adeola, S. I. Ng'ang'a, B. G. Ogunjemite, A. O. Okeyoyin, C. Roos, D. D. Wu,
815 Population genomics reveals incipient speciation, introgression, and adaptation in the
816 African mona monkey (*Cercopithecus mona*). *Mol Biol Evol* **38**, 876-890 (2021).
- 817 28. D. M. Bickhart, B. D. Rosen, S. Koren, B. L. Sayre, A. R. Hastie, S. Chan, J. Lee, E.
818 T. Lam, I. Liachko, S. T. Sullivan, J. N. Burton, H. J. Huson, J. C. Nystrom, C. M.
819 Kelley, J. L. Hutchison, Y. Zhou, J. Sun, A. Crisa, F. A. Ponce de Leon, J. C.
820 Schwartz, J. A. Hammond, G. C. Waldbieser, S. G. Schroeder, G. E. Liu, M. J.
821 Dunham, J. Shendure, T. S. Sonstegard, A. M. Phillippy, C. P. Van Tassell, T. P.
822 Smith, Single-molecule sequencing and chromatin conformation capture enable *de*
823 *novo* reference assembly of the domestic goat genome. *Nat Genet* **49**, 643-650
824 (2017).

- 825 29. B.-L. Zhang., W. Chen., Z. Wang., W. Pang., M.-T. Luo., S. Wang., Y. Shao., W.-Q.
826 He., Y. Deng., L. Zhou., J. Chen., M. Yang., Y. Wu., L. Wang., H. Fernandez., S.
827 Molloy., H. Meunier., F. Wanert., L. Kuderna., T. Marques-Bonet., C. Roos., X. Qi.,
828 M. Li., Z.-J. Liu., M. H. Schierup., D. N. Cooper., J. Liu., Y.-T. Zheng., G. Zhang.,
829 D.-D. Wu., Comparative genomics reveals the hybrid origin of a macaque group. *Sci*
830 *Adv*, accepted (2022).
- 831 30. H. Wu., Z. Wang., Y. Zhang., L. Frantz., C. Roos., D. M. Irwin., C. Zhang., X. Liu.,
832 D. Wu., S. Huang., T. Gu., J. Liu., L. Yu., Hybrid origin of a primate, the gray snub-
833 nosed monkey. *Science*, accepted (2022).
- 834 31. J. Wu., L. Zhao., L. Wang., X. Guang., P. A. Garber., C. Opie., Y. Yuan., R. Diao.,
835 G. Li., K. Wang., R. Pan., W. Ji., H. Sun., Z.-P. Huang., C. Xu., A. B. Witarto., R.
836 Jia., C. Zhang., C. Deng., Q. Qiu., G. Zhang., Cyril C. Grueter, D.-D. Wu., B. Li., X.-
837 G. Qi., Cold adaptations promoted social evolution in Asian Colobine Primate.
838 *Science*, accepted (2022).
- 839 32. Ming-Li Li, Sheng Wang, Penghui Xu, Hang-Yu Tian , Yong Shao, Zi-Jun Xiong,
840 Xiao-Guang Qi, David N. Cooper, Ya-Ping Zhang, Guojie Zhang, He Helen Zhu, D.-
841 D. Wu, Functional genomics analysis reveals the evolutionary adaptation and
842 demographic history of *pygmy lorises*. *Proc Natl Acad Sci U S A* **119**, e2123030119
843 (2022).
- 844 33. M. S. Ye, J. Y. Zhang, D. D. Yu, M. Xu, L. Xu, L. B. Lv, Q. Y. Zhu, Y. Fan, Y. G.
845 Yao, Comprehensive annotation of the Chinese tree shrew genome by large-scale
846 RNA sequencing and long-read isoform sequencing. *Zool Res* **42**, 692-709 (2021).
- 847 34. A. M. Kozlov, A. J. Aberer, A. Stamatakis, ExaML version 3: a tool for
848 phylogenomic analyses on supercomputers. *Bioinformatics* **31**, 2577-2579 (2015).
- 849 35. P. Perelman, W. E. Johnson, C. Roos, H. N. Seuánez, J. E. Horvath, M. A. Moreira,
850 B. Kessing, J. Pontius, M. Roelke, Y. Rumpler, M. P. Schneider, A. Silva, S. J.
851 O'Brien, J. Pecon-Slattey, A molecular phylogeny of living primates. *PLoS Genet* **7**,
852 e1001342 (2011).
- 853 36. C. M. Shi, Z. Yang, Coalescent-based analyses of genomic sequence data provide a
854 robust resolution of phylogenetic relationships among major groups of gibbons. *Mol*
855 *Biol Evol* **35**, 159-179 (2018).
- 856 37. A. Hobolth, O. F. Christensen, T. Mailund, M. H. Schierup, Genomic relationships
857 and speciation times of human, chimpanzee, and gorilla inferred from a coalescent
858 hidden Markov model. *PLoS Genet* **3**, e7 (2007).
- 859 38. I. Rivas-González., M. Rousselle., F. Li., L. Zhou., J. Y. Dutheil., K. Munch., Y.
860 Shao., D. Wu., M. H. Schierup., G. Zhang., Pervasive incomplete lineage sorting
861 illuminates speciation and selection processes in primates. *Science*, under review
862 (2022).
- 863 39. D. Vanderpool, B. Q. Minh, R. Lanfear, D. Hughes, S. Murali, R. A. Harris, M.
864 Raveendran, D. M. Muzny, M. S. Hibbins, R. J. Williamson, Primate phylogenomics
865 uncovers multiple rapid radiations and ancient interspecific introgression. *PLoS Biol*
866 **18**, e3000954 (2020).
- 867 40. Z. Yang, PAML 4: phylogenetic analysis by maximum likelihood. *Mol Biol Evol* **24**,
868 1586-1591 (2007).

- 869 41. S. Alvarez-Carretero, A. U. Tamuri, M. Battini, F. F. Nascimento, E. Carlisle, R. J.
870 Asher, Z. Yang, P. C. J. Donoghue, M. Dos Reis, A species-level timeline of mammal
871 evolution integrating phylogenomic data. *Nature* **602**, 263-267 (2022).
- 872 42. C. Liu, J. Gao, X. Cui, Z. Li, L. Chen, Y. Yuan, Y. Zhang, L. Mei, L. Zhao, D. Cai,
873 M. Hu, B. Zhou, Z. Li, T. Qin, H. Si, G. Li, Z. Lin, Y. Xu, C. Zhu, Y. Yin, C. Zhang,
874 W. Xu, Q. Li, K. Wang, M. T. P. Gilbert, R. Heller, W. Wang, J. Huang, Q. Qiu, A
875 towering genome: Experimentally validated adaptations to high blood pressure and
876 extreme stature in the giraffe. *Sci Adv* **7**, eabe9459 (2021).
- 877 43. E. E. Eichler, D. Sankoff, Structural dynamics of eukaryotic chromosome evolution.
878 *Science* **301**, 793-797 (2003).
- 879 44. Y. Yin, H. Fan, B. Zhou, Y. Hu, G. Fan, J. Wang, F. Zhou, W. Nie, C. Zhang, L. Liu,
880 Z. Zhong, W. Zhu, G. Liu, Z. Lin, C. Liu, J. Zhou, G. Huang, Z. Li, J. Yu, Y. Zhang,
881 Y. Yang, B. Zhuo, B. Zhang, J. Chang, H. Qian, Y. Peng, X. Chen, L. Chen, Z. Li, Q.
882 Zhou, W. Wang, F. Wei, Molecular mechanisms and topological consequences of
883 drastic chromosomal rearrangements of muntjac deer. *Nat Commun* **12**, 6858 (2021).
- 884 45. R. Stanyon, M. Rocchi, O. Capozzi, R. Roberto, D. Misceo, M. Ventura, M. F.
885 Cardone, F. Bigoni, N. Archidiacono, Primate chromosome evolution: ancestral
886 karyotypes, marker order and neocentromeres. *Chromosome Res* **16**, 17-39 (2008).
- 887 46. T. Marques-Bonet, J. M. Kidd, M. Ventura, T. A. Graves, Z. Cheng, L. W. Hillier, Z.
888 Jiang, C. Baker, R. Malfavon-Borja, L. A. Fulton, C. Alkan, G. Aksay, S. Girirajan,
889 P. Siswara, L. Chen, M. F. Cardone, A. Navarro, E. R. Mardis, R. K. Wilson, E. E.
890 Eichler, A burst of segmental duplications in the genome of the African great ape
891 ancestor. *Nature* **457**, 877-881 (2009).
- 892 47. P. D. Stenson., M. Mort., E. V. Ball., M. Chapman., K. Evans., L. Azevedo., M.
893 Hayden., S. Heywood., D. S. Millar., A. D. Phillips., D. N. Cooper., The Human
894 Gene Mutation Database (HGMD[®]): optimizing its use in a clinical diagnostic or
895 research setting. *Hum Genet* **139**, 1197-1207 (2020).
- 896 48. L. Chen, Q. Qiu, Y. Jiang, K. Wang, Z. Lin, Z. Li, F. Bibi, Y. Yang, J. Wang, W. Nie,
897 W. Su, G. Liu, Q. Li, W. Fu, X. Pan, C. Liu, J. Yang, C. Zhang, Y. Yin, Y. Wang, Y.
898 Zhao, C. Zhang, Z. Wang, Y. Qin, W. Liu, B. Wang, Y. Ren, R. Zhang, Y. Zeng, R.
899 R. da Fonseca, B. Wei, R. Li, W. Wan, R. Zhao, W. Zhu, Y. Wang, S. Duan, Y. Gao,
900 Y. E. Zhang, C. Chen, C. Hvilsom, C. W. Epps, L. G. Chemnick, Y. Dong, S.
901 Mirarab, H. R. Siegismund, O. A. Ryder, M. T. P. Gilbert, H. A. Lewin, G. Zhang, R.
902 Heller, W. Wang, Large-scale ruminant genome sequencing provides insights into
903 their evolution and distinct traits. *Science* **364**, eaav6202 (2019).
- 904 49. J. D. Smith, J. W. Bickham, T. R. Gregory, Patterns of genome size diversity in bats
905 (order Chiroptera). *Genome* **56**, 457-472 (2013).
- 906 50. S. Shen, L. Lin, J. J. Cai, P. Jiang, E. J. Kenkel, M. R. Stroik, S. Sato, B. L. Davidson,
907 Y. Xing, Widespread establishment and regulatory impact of Alu exons in human
908 genes. *Proc Natl Acad Sci U S A* **108**, 2837-2842 (2011).
- 909 51. G. E. Liu, C. Alkan, L. Jiang, S. Zhao, E. E. Eichler, Comparative analysis of Alu
910 repeats in primate genomes. *Genome Res* **19**, 876-885 (2009).

- 911 52. T. Hayakawa, Y. Satta, P. Gagneux, A. Varki, N. Takahata, Alu-mediated
912 inactivation of the human CMP-*N*-acetylneuraminic acid hydroxylase gene. *Proc Natl*
913 *Acad Sci U S A* **98**, 11399-11404 (2001).
- 914 53. P. Kuehnen, M. Mischke, S. Wiegand, C. Sers, B. Horsthemke, S. Lau, T. Keil, Y. A.
915 Lee, A. Grueters, H. Krude, An Alu element-associated hypermethylation variant of
916 the *POMC* gene is associated with childhood obesity. *PLoS Genet* **8**, e1002543
917 (2012).
- 918 54. J. Jurka, Evolutionary impact of human Alu repetitive elements. *Curr Opin Genet*
919 *Dev* **14**, 603-608 (2004).
- 920 55. G. Zhang, C. Li, Q. Li, B. Li, D. M. Larkin, C. Lee, J. F. Storz, A. Antunes, M. J.
921 Greenwold, R. W. Meredith, A. Ödeen, J. Cui, Q. Zhou, L. Xu, H. Pan, Z. Wang, L.
922 Jin, P. Zhang, H. Hu, W. Yang, J. Hu, J. Xiao, Z. Yang, Y. Liu, Q. Xie, H. Yu, J.
923 Lian, P. Wen, F. Zhang, H. Li, Y. Zeng, Z. Xiong, S. Liu, L. Zhou, Z. Huang, N. An,
924 J. Wang, Q. Zheng, Y. Xiong, G. Wang, B. Wang, J. Wang, Y. Fan, R. R. da
925 Fonseca, A. Alfaro-Núñez, M. Schubert, L. Orlando, T. Mourier, J. T. Howard, G.
926 Ganapathy, A. Pfenning, O. Whitney, M. V. Rivas, E. Hara, J. Smith, M. Farré, J.
927 Narayan, G. Slavov, M. N. Romanov, R. Borges, J. P. Machado, I. Khan, M. S.
928 Springer, J. Gatesy, F. G. Hoffmann, J. C. Opazo, O. Håstad, R. H. Sawyer, H. Kim,
929 K. W. Kim, H. J. Kim, S. Cho, N. Li, Y. Huang, M. W. Bruford, X. Zhan, A. Dixon,
930 M. F. Bertelsen, E. Derryberry, W. Warren, R. K. Wilson, S. Li, D. A. Ray, R. E.
931 Green, S. J. O'Brien, D. Griffin, W. E. Johnson, D. Haussler, O. A. Ryder, E.
932 Willerslev, G. R. Graves, P. Alström, J. Fjeldså, D. P. Mindell, S. V. Edwards, E. L.
933 Braun, C. Rahbek, D. W. Burt, P. Houde, Y. Zhang, H. Yang, J. Wang, E. D. Jarvis,
934 M. T. Gilbert, J. Wang, Comparative genomics reveals insights into avian genome
935 evolution and adaptation. *Science* **346**, 1311-1320 (2014).
- 936 56. P. Moorjani, C. E. Amorim, P. F. Arndt, M. Przeworski, Variation in the molecular
937 clock of primates. *Proc Natl Acad Sci U S A* **113**, 10607-10612 (2016).
- 938 57. E. Fontanillas, J. J. Welch, J. A. Thomas, L. Bromham, The influence of body size
939 and net diversification rate on molecular evolution during the radiation of animal
940 phyla. *BMC Evol Biol* **7**, 95 (2007).
- 941 58. A. Wong, Covariance between testes size and substitution rates in primates. *Mol Biol*
942 *Evol* **31**, 1432-1436 (2014).
- 943 59. W. H. Li, M. Tanimura, The molecular clock runs more slowly in man than in apes
944 and monkeys. *Nature* **326**, 93-96 (1987).
- 945 60. M. E. Steiper, N. M. Young, Primate molecular divergence dates. *Mol Phylogenet*
946 *Evol* **41**, 384-394 (2006).
- 947 61. S. H. Kim, N. Elango, C. Warden, E. Vigoda, S. V. Yi, Heterogeneous genomic
948 molecular clocks in primates. *PLoS Genet* **2**, e163 (2006).
- 949 62. J. Schmitz, A. Noll, C. A. Raabe, G. Churakov, R. Voss, M. Kiefmann, T.
950 Rozhdestvensky, J. Brosius, R. Baertsch, H. Clawson, C. Roos, A. Zimin, P. Minx,
951 M. J. Montague, R. K. Wilson, W. C. Warren, Genome sequence of the basal
952 haplorrhine primate *Tarsius syrichta* reveals unusual insertions. *Nat Commun* **7**,
953 12997 (2016).

- 954 63. L. Fang, W. Cai, S. Liu, O. Canela-Xandri, Y. Gao, J. Jiang, K. Rawlik, B. Li, S. G.
 955 Schroeder, B. D. Rosen, C. J. Li, T. S. Sonstegard, L. J. Alexander, C. P. Van Tassell,
 956 P. M. VanRaden, J. B. Cole, Y. Yu, S. Zhang, A. Tenesa, L. Ma, G. E. Liu,
 957 Comprehensive analyses of 723 transcriptomes enhance genetic and biological
 958 interpretations for complex traits in cattle. *Genome Res* **30**, 790-801 (2020).
- 959 64. B. Y. Liao, J. Zhang, Low rates of expression profile divergence in highly expressed
 960 genes and tissue-specific genes during mammalian evolution. *Mol Biol Evol* **23**,
 961 1119-1128 (2006).
- 962 65. G. J. Wyckoff, W. Wang, C. I. Wu, Rapid evolution of male reproductive genes in the
 963 descent of man. *Nature* **403**, 304-309 (2000).
- 964 66. T. Boehm, Evolution of vertebrate immunity. *Curr Biol* **22**, R722-R732 (2012).
- 965 67. H. Y. Wang, H. C. Chien, N. Osada, K. Hashimoto, S. Sugano, T. Gojobori, C. K.
 966 Chou, S. F. Tsai, C. I. Wu, C. K. Shen, Rate of evolution in brain-expressed genes in
 967 humans and other primates. *PLoS Biol* **5**, e13 (2007).
- 968 68. Materials and methods are available as Supplementary Material.
- 969 69. J. Tohyama, M. Nakashima, S. Nabatame, C. n. Gaik-Siew, R. Miyata, Z. Rener-
 970 Primec, M. Kato, N. Matsumoto, H. Saito, *SPTANI* encephalopathy: distinct
 971 phenotypes and genotypes. *J Hum Genet* **60**, 167-173 (2015).
- 972 70. P. Mansfield, J. N. Constantino, D. Baldrige, *MYTIL*: A systematic review of
 973 genetic variation encompassing schizophrenia and autism. *Am J Med Genet B*
 974 *Neuropsychiatr Genet* **183**, 227-233 (2020).
- 975 71. M. Maekawa, T. Ohnishi, K. Hashimoto, A. Watanabe, Y. Iwayama, H. Ohba, E.
 976 Hattori, K. Yamada, T. Yoshikawa, Analysis of strain-dependent prepulse inhibition
 977 points to a role for Shmt1 (*SHMT1*) in mice and in schizophrenia. *J Neurochem* **115**,
 978 1374-1385 (2010).
- 979 72. X. Bi., L. Zhou., J.-J. Zhang., S. Feng., M. Hu., D. N. Cooper., J. Lin., J. Li., D.-D.
 980 Wu., G. Zhang., Lineage-specific accelerated sequences underlying primate
 981 evolution. *Sci adv*, under review (2022).
- 982 73. J. K. Rilling, T. R. Insel, Differential expansion of neural projection systems in
 983 primate brain evolution. *Neuroreport* **10**, 1453-1459 (1999).
- 984 74. K. Isler, E. Christopher Kirk, J. M. Miller, G. A. Albrecht, B. R. Gelvin, R. D.
 985 Martin, Endocranial volumes of primate species: scaling analyses using a
 986 comprehensive and reliable data set. *J Hum Evol* **55**, 967-978 (2008).
- 987 75. C. Plachez, L. J. Richards, Mechanisms of axon guidance in the developing nervous
 988 system. *Curr Top Dev Biol* **69**, 267-346 (2005).
- 989 76. M. A. Robichaux, C. W. Cowan, Signaling mechanisms of axon guidance and early
 990 synaptogenesis. *Curr Top Behav Neurosci* **16**, 19-48 (2014).
- 991 77. J. Falk, A. Bechara, R. Fiore, H. Nawabi, H. Zhou, C. Hoyo-Becerra, M. Bozon, G.
 992 Rougon, M. Grumet, A. W. Puschel, J. R. Sanes, V. Castellani, Dual functional
 993 activity of semaphorin 3B is required for positioning the anterior commissure.
 994 *Neuron* **48**, 63-75 (2005).
- 995 78. M. A. Wolman, Y. Liu, H. Tawarayama, W. Shoji, M. C. Halloran, Repulsion and
 996 attraction of axons by semaphorin3D are mediated by different neuropilins in vivo. *J*
 997 *Neurosci* **24**, 8428-8435 (2004).

- 998 79. C. Kudo, I. Ajioka, Y. Hirata, K. Nakajima, Expression profiles of *EPHA3* at both the
999 RNA and protein level in the developing mammalian forebrain. *J Comp Neurol* **487**,
1000 255-269 (2005).
- 1001 80. M. V. Tejada-Simon, Modulation of actin dynamics by *RAC1* to target cognitive
1002 function. *J Neurochem* **133**, 767-779 (2015).
- 1003 81. S. L. Eastwood, P. J. Harrison, Decreased mRNA Expression of Netrin-G1 and
1004 Netrin-G2 in the Temporal Lobe in Schizophrenia and Bipolar Disorder.
1005 *Neuropsychopharmacology* **33**, 933-945 (2008).
- 1006 82. D. Pan, Hippo signaling in organ size control. *Genes Dev* **21**, 886-897 (2007).
- 1007 83. S. H. Patel, F. D. Camargo, D. Yimlamai, Hippo signaling in the liver regulates organ
1008 size, cell fate, and carcinogenesis. *Gastroenterology* **152**, 533-545 (2017).
- 1009 84. R. H. Gokhale, A. W. Shingleton, Size control: the developmental physiology of
1010 body and organ size regulation. *Wiley Interdiscip Rev Dev Biol* **4**, 335-356 (2015).
- 1011 85. E. C. Kirk, Comparative morphology of the eye in primates. *Anat Rec A Discov Mol*
1012 *Cell Evol Biol* **281**, 1095-1103 (2004).
- 1013 86. A. C. Wiik, C. Wade, T. Biagi, E. O. Ropstad, E. Bjerkas, K. Lindblad-Toh, F.
1014 Lingaas, A deletion in nephronophthisis 4 (*NPHP4*) is associated with recessive
1015 cone-rod dystrophy in standard wire-haired dachshund. *Genome Res* **18**, 1415-1421
1016 (2008).
- 1017 87. P. Liskova, L. Dudakova, C. J. Evans, K. E. Rojas Lopez, N. Pontikos, D.
1018 Athanasiou, H. Jama, J. Sach, P. Skalicka, V. Stranecky, S. Kmoch, C. Thaug, M.
1019 Filipec, M. E. Cheetham, A. E. Davidson, S. J. Tuft, A. J. Hardcastle, Ectopic *GRHL2*
1020 expression due to non-coding mutations promotes cell state transition and causes
1021 posterior polymorphous corneal dystrophy 4. *Am J Hum Genet* **102**, 447-459 (2018).
- 1022 88. Y. Toda, T. Hayakawa, A. Itoigawa, Y. Kurihara, T. Nakagita, M. Hayashi, R.
1023 Ashino, A. D. Melin, Y. Ishimaru, S. Kawamura, H. Imai, T. Misaka, Evolution of
1024 the primate glutamate taste sensor from a nucleotide sensor. *Curr Biol* **31**, 4641-
1025 4649.e4645 (2021).
- 1026 89. J. M. Kamilar, B. J. Bradley, Interspecific variation in primate coat colour supports
1027 Gloger's rule. *J Biogeogr* **38**, 2270-2277 (2011).
- 1028 90. S. Hu, Y. Chen, B. Zhao, N. Yang, S. Chen, J. Shen, G. Bao, X. Wu, *KIT* is involved
1029 in melanocyte proliferation, apoptosis and melanogenesis in the rex rabbit. *PeerJ* **8**,
1030 e9402 (2020).
- 1031 91. M. C. Garrido, B. C. Bastian, *KIT* as a therapeutic target in melanoma. *J Invest*
1032 *Dermatol* **130**, 20-27 (2010).
- 1033 92. J. M. Grichnik, *KIT* and melanocyte migration. *J Invest Dermatol* **126**, 945-947
1034 (2006).
- 1035 93. Y. Mizutani, N. Hayashi, M. Kawashima, G. Imokawa, A single UVB exposure
1036 increases the expression of functional *KIT* in human melanocytes by up-regulating
1037 *MITF* expression through the phosphorylation of p38/CREB. *Arch Dermatol Res* **302**,
1038 283-294 (2010).
- 1039 94. R. Kitamura, K. Tsukamoto, K. Harada, A. Shimizu, S. Shimada, T. Kobayashi, G.
1040 Imokawa, Mechanisms underlying the dysfunction of melanocytes in vitiligo

- 1041 epidermis: role of SCF/KIT protein interactions and the downstream effector, MITF-
1042 M. *J Pathol* **202**, 463-475 (2004).
- 1043 95. B. Wen, Y. Chen, H. Li, J. Wang, J. Shen, A. Ma, J. Qu, K. Bismuth, J. Debbache, H.
1044 Arnheiter, L. Hou, Allele-specific genetic interactions between *Mitf* and *Kit* affect
1045 melanocyte development. *Pigment Cell Melanoma Res* **23**, 441-447 (2010).
- 1046 96. D. L. C. van den Berg, R. Azzarelli, K. Oishi, B. Martynoga, N. Urban, D. H. W.
1047 Dekkers, J. A. Demmers, F. Guillemot, *NIPBL* interacts with *ZFP609* and the
1048 integrator complex to regulate cortical neuron migration. *Neuron* **93**, 348-361 (2017).
- 1049 97. G. H. Mochida, C. A. Walsh, Molecular genetics of human microcephaly. *Curr Opin*
1050 *Neurol* **14**, 151-156 (2001).
- 1051 98. S. H. Montgomery, I. Capellini, C. Venditti, R. A. Barton, N. I. Mundy, Adaptive
1052 evolution of four microcephaly genes and the evolution of brain size in Anthropoid
1053 primates. *Mol Biol Evol* **28**, 625-638 (2010).
- 1054 99. L. Shi, M. Li, Q. Lin, X. Qi, B. Su, Functional divergence of the brain-size regulating
1055 gene *MCPHI* during primate evolution and the origin of humans. *BMC Biol* **11**, 62
1056 (2013).
- 1057 100. L. Shi, B. Su, A transgenic monkey model for the study of human brain evolution.
1058 *Zool Res* **40**, 236-238 (2019).
- 1059 101. J. Rogers, P. Kochunov, K. Zilles, W. Shelledy, J. Lancaster, P. Thompson, R.
1060 Duggirala, J. Blangero, P. T. Fox, D. C. Glahn, On the genetic architecture of cortical
1061 folding and brain volume in primates. *Neuroimage* **53**, 1103-1108 (2010).
- 1062 102. S. V. Puram, A. Riccio, S. Koirala, Y. Ikeuchi, A. H. Kim, G. Corfas, A. Bonni, A
1063 TRPC5-regulated calcium signaling pathway controls dendrite patterning in the
1064 mammalian brain. *Genes Dev* **25**, 2659-2673 (2011).
- 1065 103. A. Yamada, E. Inoue, M. Deguchi-Tawarada, C. Matsui, A. Togawa, T. Nakatani, Y.
1066 Ono, Y. Takai, *NECL-2/CADM1* interacts with *ERBB4* and regulates its activity in
1067 GABAergic neurons. *Mol Cell Neurosci* **56**, 234-243 (2013).
- 1068 104. R. Kusano, K. Fujita, Y. Shinoda, Y. Nagaura, H. Kiyonari, T. Abe, T. Watanabe, Y.
1069 Matsui, M. Fukaya, H. Sakagami, T. Sato, J.-i. Funahashi, M. Ohnishi, S. Tamura, T.
1070 Kobayashi, Targeted disruption of the mouse protein phosphatase *PPM1L* gene leads
1071 to structural abnormalities in the brain. *FEBS Letters* **590**, 3606-3615 (2016).
- 1072 105. M. Talarowska, J. Szemraj, M. Kowalczyk, P. Gałeczki, Serum *KIBRA* mRNA and
1073 protein expression and cognitive functions in depression. *Med Sci Monit* **22**, 152-160
1074 (2016).
- 1075 106. A. K. Pandey, L. Lu, X. Wang, R. Homayouni, R. W. Williams, Functionally
1076 enigmatic genes: a case study of the brain ignorome. *PLoS One* **9**, e88889 (2014).
- 1077 107. A. Graziano, G. Foffani, E. B. Knudsen, J. Shumsky, K. A. Moxon, Passive exercise
1078 of the hind limbs after complete thoracic transection of the spinal cord promotes
1079 cortical reorganization. *PLoS One* **8**, e54350 (2013).
- 1080 108. H. Li, J. C. Radford, M. J. Ragusa, K. L. Shea, S. R. McKercher, J. D. Zaremba, W.
1081 Soussou, Z. Nie, Y. J. Kang, N. Nakanishi, S. Okamoto, A. J. Roberts, J. J. Schwarz,
1082 S. A. Lipton, Transcription factor *MEF2C* influences neural stem/progenitor cell
1083 differentiation and maturation *in vivo*. *Proc Natl Acad Sci U S A* **105**, 9397-9402
1084 (2008).

- 1085 109. Y. Chang, O. Klezovitch, R. S. Walikonis, V. Vasioukhin, J. J. LoTurco, Discs large
1086 5 is required for polarization of citron kinase in mitotic neural precursors. *Cell Cycle*
1087 **9**, 1990-1997 (2010).
- 1088 110. M. R. Sarkisian, Discs large 5: a new regulator of Citron kinase localization in
1089 developing neocortex: comment on: Chang Y, et al. *Cell Cycle* 2010; 9:1990-7. *Cell*
1090 *Cycle* **9**, 1876 (2010).
- 1091 111. D. A. Berg, L. Belnoue, H. Song, A. Simon, Neurotransmitter-mediated control of
1092 neurogenesis in the adult vertebrate brain. *Development* **140**, 2548-2561 (2013).
- 1093 112. P. Levitt, J. A. Harvey, E. Friedman, K. Simansky, E. H. Murphy, New evidence for
1094 neurotransmitter influences on brain development. *Trends Neurosci* **20**, 269-274
1095 (1997).
- 1096 113. L. Wang, X. You, S. Lotinun, L. Zhang, N. Wu, W. Zou, Mechanical sensing protein
1097 PIEZO1 regulates bone homeostasis via osteoblast-osteoclast crosstalk. *Nat Commun*
1098 **11**, 282 (2020).
- 1099 114. M. Linder, M. Hecking, E. Glitzner, K. Zwerina, M. Holcman, L. Bakiri, M. G.
1100 Ruocco, J. Tuckermann, G. Schett, E. F. Wagner, M. Sibilica, *EGFR* controls bone
1101 development by negatively regulating mTOR-signaling during osteoblast
1102 differentiation. *Cell Death Differ* **25**, 1094-1106 (2018).
- 1103 115. F. Xiao, C. Wang, C. Wang, Y. Gao, X. Zhang, X. Chen, *BMPER* enhances bone
1104 formation by promoting the osteogenesis-angiogenesis coupling process in
1105 mesenchymal stem cells. *Cell Physiol Biochem* **45**, 1927-1939 (2018).
- 1106 116. S. Zanotti, E. Canalis, *NOTCH1* and *NOTCH2* expression in osteoblast precursors
1107 regulates femoral microarchitecture. *Bone* **62**, 22-28 (2014).
- 1108 117. J. M. Kim, C. Lin, Z. Stavre, M. B. Greenblatt, J. H. Shim, Osteoblast-osteoclast
1109 communication and bone homeostasis. *Cells* **9**, 2073 (2020).
- 1110 118. S. Zanotti, E. Canalis, Notch signaling and the skeleton. *Endocr Rev* **37**, 223-253
1111 (2016).
- 1112 119. M. Schmidt, Locomotion and postural behaviour. *Adv Sci Res* **5**, 23-39 (2011).
- 1113 120. Y. He, X. Luo, B. Zhou, T. Hu, X. Meng, P. A. Audano, Z. N. Kronenberg, E. E.
1114 Eichler, J. Jin, Y. Guo, Y. Yang, X. Qi, B. Su, Long-read assembly of the Chinese
1115 rhesus macaque genome and identification of ape-specific structural variants. *Nat*
1116 *Commun* **10**, 4233 (2019).
- 1117 121. S. A. Williams, G. A. Russo, Evolution of the hominoid vertebral column: the long
1118 and the short of it. *Evol Anthropol* **24**, 15-32 (2015).
- 1119 122. K. Semba, K. Araki, Z. Li, K. Matsumoto, M. Suzuki, N. Nakagata, K. Takagi, M.
1120 Takeya, K. Yoshinobu, M. Araki, K. Imai, K. Abe, K. Yamamura, A novel murine
1121 gene, sickle tail, linked to the Danforth's short tail locus, is required for normal
1122 development of the intervertebral disc. *Genetics* **172**, 445-456 (2006).
- 1123 123. N. Al Dhaheri, N. Wu, S. Zhao, Z. Wu, R. D. Blank, J. Zhang, C. Raggio, M.
1124 Halanski, J. Shen, K. Noonan, G. Qiu, B. Nemeth, S. Sund, S. L. Dunwoodie, G.
1125 Chapman, I. Glurich, R. D. Steiner, E. Wohler, R. Martin, N. L. Sobreira, P. F.
1126 Giampietro, *KIAA1217*: a novel candidate gene associated with isolated and
1127 syndromic vertebral malformations. *Am J Med Genet A* **182**, 1664-1672 (2020).

- 1128 124. J. R. Usherwood, J. E. Bertram, Understanding brachiation: insight from a collisional
1129 perspective. *J Exp Biol* **206**, 1631-1642 (2003).
- 1130 125. J. R. Usherwood, S. G. Larson, J. E. Bertram, Mechanisms of force and power
1131 production in unsteady ricochet brachiation. *Am J Phys Anthropol* **120**, 364-372
1132 (2003).
- 1133 126. S. M. Cheyne, in *Primate locomotion: linking field and laboratory research*, K.
1134 D'Août, E. E. Vereecke, Eds. (Springer New York, New York, NY, 2011), pp. 201-
1135 213.
- 1136 127. C. Thiel, K. Kessler, A. Giessl, A. Dimmler, S. A. Shalev, S. von der Haar, M.
1137 Zenker, D. Zahnleiter, H. Stoss, E. Beinder, R. Abou Jamra, A. B. Ekici, N. Schroder-
1138 Kress, T. Aigner, T. Kirchner, A. Reis, J. H. Brandstatter, A. Rauch, *NEK1* mutations
1139 cause short-rib polydactyly syndrome type majewski. *Am J Hum Genet* **88**, 106-114
1140 (2011).
- 1141 128. J. El Hokayem, C. Huber, A. Couvé, J. Aziza, G. Baujat, R. Bouvier, D. P.
1142 Cavalcanti, F. A. Collins, M.-P. Cordier, A.-L. Delezoide, M. Gonzales, D. Johnson,
1143 M. Le Merrer, A. Levy-Mozziconacci, P. Loget, D. Martin-Coignard, J. Martinovic,
1144 G. R. Mortier, M.-J. Perez, J. Roume, G. Scarano, A. Munnich, V. Cormier-Daire,
1145 *NEK1* and *DYNC2H1* are both involved in short rib polydactyly Majewski type but
1146 not in Beemer Langer cases. *J Med Genet* **49**, 227-233 (2012).
- 1147 129. J. M. Vazquez, V. J. Lynch, Pervasive duplication of tumor suppressors in
1148 Afrotherians during the evolution of large bodies and reduced cancer risk. *Elife* **10**,
1149 (2021).
- 1150 130. J. G. M. Thewissen, L. N. Cooper, J. C. George, S. Bajpai, From land to water: the
1151 origin of whales, dolphins, and porpoises. *Evo Edu Outreach* **2**, 272-288 (2009).
- 1152 131. W. L. Jungers, in *Size and scaling in primate biology*, W. L. Jungers, Ed. (Springer
1153 US, Boston, MA, 1985), pp. 345-381.
- 1154 132. A. M. Rudolf, Q. Wu, L. Li, J. Wang, Y. Huang, J. Togo, C. Liechti, M. Li, C. Niu,
1155 Y. Nie, F. Wei, J. R. Speakman, A single nucleotide mutation in the dual-oxidase 2
1156 (*DUOX2*) gene causes some of the panda's unique metabolic phenotypes. *Natl Sci Rev*
1157 **9**, nwab125 (2022).
- 1158 133. K. R. Johnson, C. C. Marden, P. Ward-Bailey, L. H. Gagnon, R. T. Bronson, L. R.
1159 Donahue, Congenital hypothyroidism, dwarfism, and hearing impairment caused by a
1160 missense mutation in the mouse dual oxidase 2 gene, *Duox2*. *Mol Endocrinol* **21**,
1161 1593-1602 (2007).
- 1162 134. J. G. Fleagle, *Primate adaptation and evolution*. (Academic press, 2013).
- 1163 135. K. Milton, Physiological ecology of howlers (*Alouatta*): energetic and digestive
1164 considerations and comparison with the Colobinae. *Int J Primatol* **19**, 513-548
1165 (1998).
- 1166 136. I. Matsuda, C. A. Chapman, M. Clauss, Colobine forestomach anatomy and diet. *J*
1167 *Morphol* **280**, 1608-1616 (2019).
- 1168 137. M. C. Janiak, Digestive enzymes of human and nonhuman primates. *Evol Anthropol*
1169 **25**, 253-266 (2016).

1170 138. J. J. Kim, R. Miura, Acyl-CoA dehydrogenases and acyl-CoA oxidases. Structural
1171 basis for mechanistic similarities and differences. *Eur J Biochem* **271**, 483-493
1172 (2004).

1173 139. C. Matziouridou, S. D. C. Rocha, O. A. Haabeth, K. Rudi, H. Carlsen, A. Kielland,
1174 iNOS- and NOX1-dependent ROS production maintains bacterial homeostasis in the
1175 ileum of mice. *Mucosal Immunol* **11**, 774-784 (2018).

1176 140. C.-J. Li, R. W. Li, R. L. Baldwin Vi, Assembly and analysis of changes in
1177 transcriptomes of dairy cattle rumen epithelia during lactation and dry periods. *Agric
1178 Sci* **9**, 619-638 (2018).

1179 141. M. C. Janiak, A. S. Burrell, J. D. Orkin, T. R. Disotell, Duplication and parallel
1180 evolution of the pancreatic ribonuclease gene (*RNASE1*) in folivorous non-colobine
1181 primates, the howler monkeys (*Alouatta spp.*). *Sci Rep* **9**, 20366 (2019).

1182 142. P. Pontarotti, *Evolutionary biology-mechanisms and trends*. (Springer Science &
1183 Business Media, 2012).

1184 143. N. J. Dominy, P. W. Lucas, Ecological importance of trichromatic vision to primates.
1185 *Nature* **410**, 363-366 (2001).

1186 144. N. G. Caine, N. I. Mundy, Demonstration of a foraging advantage for trichromatic
1187 marmosets (*Callithrix geoffroyi*) dependent on food colour. *Proc Biol Sci* **267**, 439-
1188 444 (2000).

1189 145. A. C. Smith, H. M. Buchanan-Smith, A. K. Surridge, D. Osorio, N. I. Mundy, The
1190 effect of colour vision status on the detection and selection of fruits by tamarins
1191 (*Saguinus spp.*). *J Exp Biol* **206**, 3159-3165 (2003).

1192 146. S. Heritage, Modeling olfactory bulb evolution through primate phylogeny. *PLoS
1193 One* **9**, e113904 (2014).

1194 147. A. Matsui, Y. Go, Y. Niimura, Degeneration of olfactory receptor gene repertoires in
1195 primates: no direct link to full trichromatic vision. *Mol Biol Evol* **27**, 1192-1200
1196 (2010).

1197 148. T. D. Smith, K. P. Bhatnagar, Microsmatic primates: reconsidering how and when
1198 size matters. *Anat Rec B New Anat* **279**, 24-31 (2004).

1199 149. A. Berghard, A. C. Hagglund, S. Bohm, L. Carlsson, *LHX2*-dependent specification
1200 of olfactory sensory neurons is required for successful integration of olfactory,
1201 vomeronasal, and GnRH neurons. *FASEB J* **26**, 3464-3472 (2012).

1202 150. J. Hirota, P. Mombaerts, The LIM-homeodomain protein LHX2 is required for
1203 complete development of mouse olfactory sensory neurons. *Proc Natl Acad Sci U S A*
1204 **101**, 8751-8755 (2004).

1205 151. H. Li, R. Durbin, Inference of human population history from individual whole-
1206 genome sequences. *Nature* **475**, 493-496 (2011).

1207 152. A. D. Barnosky, P. L. Koch, R. S. Feranec, S. L. Wing, A. B. Shabel, Assessing the
1208 causes of late Pleistocene extinctions on the continents. *Science* **306**, 70-75 (2004).

1209 153. X. Luo, Y. Liu, D. Dang, T. Hu, Y. Hou, X. Meng, F. Zhang, T. Li, C. Wang, M. Li,
1210 H. Wu, Q. Shen, Y. Hu, X. Zeng, X. He, L. Yan, S. Zhang, C. Li, B. Su, 3D Genome
1211 of macaque fetal brain reveals evolutionary innovations during primate
1212 corticogenesis. *Cell* **184**, 723-740.e721 (2021).

- 1213 154. C. Yang, Y. Zhou, S. Marcus, G. Formenti, L. A. Bergeron, Z. Song, X. Bi, J.
1214 Bergman, M. M. C. Rousselle, C. Zhou, L. Zhou, Y. Deng, M. Fang, D. Xie, Y. Zhu,
1215 S. Tan, J. Mountcastle, B. Haase, J. Balacco, J. Wood, W. Chow, A. Rhie, M. Pippel,
1216 M. M. Fabiszak, S. Koren, O. Fedrigo, W. A. Freiwald, K. Howe, H. Yang, A. M.
1217 Phillippy, M. H. Schierup, E. D. Jarvis, G. Zhang, Evolutionary and biomedical
1218 insights from a marmoset diploid genome assembly. *Nature* **594**, 227-233 (2021).
- 1219 155. G. Dumas, S. Malesys, T. Bourgeron, Systematic detection of brain protein-coding
1220 genes under positive selection during primate evolution and their roles in cognition.
1221 *Genome Res* **31**, 484-496 (2021).
- 1222 156. J. K. Rilling, Human and nonhuman primate brains: are they allometrically scaled
1223 versions of the same design? *Evol Anthropol* **15**, 65-77 (2006).
- 1224 157. H. Stephan, H. Frahm, G. Baron, New and revised data on volumes of brain
1225 structures in insectivores and primates. *Folia Primatol (Basel)* **35**, 1-29 (1981).
- 1226

1227 **Acknowledgments**

1228 We are grateful to the many individuals in our host institutions who have provided support for
1229 this project.

1230

1231 **Funding**

1232 This work was supported by the Strategic Priority Research Program of the Chinese Academy
1233 of Sciences (XDPB17, XDB31020000), the National Natural Science Foundation of China
1234 (31822048 and 32270500), Yunnan Fundamental Research Project (2019FI010), the Animal
1235 Branch of the Germplasm Bank of Wild Species of Chinese Academy of Science (the Large
1236 Research Infrastructure Funding), International Partnership Program of Chinese Academy of
1237 Sciences (No. 152453KYSB20170002). This work was also partially supported by a Villum
1238 Investigator Grant (No. 25900) to G.Z. T.M.B. was supported by funding from the European
1239 Research Council (ERC) under the European Union's Horizon 2020 research and innovation
1240 programme (grant agreement No. 864203), BFU2017-86471-P (MINECO/FEDER, UE) and
1241 Howard Hughes International Early Career.

1242

1243 **Author contributions**

1244 D.D.W. and G.J.Z. led the project. D.D.W., G.J.Z., X.G.Q. conceived and designed the
1245 research. D.D.W., G.J.Z. and Y.S. wrote the manuscript. Y.S. drafted the manuscript. Y.S.,
1246 L.Z., F.L., L.Z., B.L.Z., F.S., J.W.C., C.Y.C., X.P.B., X.L.Z., H.L.Z., I.R.G., S.W., Y.M.W.,
1247 L.K., G.L., H.M.L., Y.L., and P.D.S. performed comparative genomics analysis. L.Z., J.H,
1248 Z.Y.S, X.L., D.P.W., and K.F. contributed genome sequencing, assembly and annotation.
1249 P.F.F., M.L., Z.J.L., G.P.T., A.D.Y., C.R., T.H., T.M.B., and J.R. collected samples. J.R. and
1250 T.M.B. generated some genome assemblies for our comparative genomics analysis. C.R.,
1251 G.P.T., J.R., L.Y., M.H.S., D.N.C., Y.G.Y., Y.P.Z., W.W. and X.G.Q. provided comments for
1252 improving the manuscript. Y.S., X.G.Q., and L.Z. plotted and revised figures. D.N.C.
1253 polished the manuscript. All authors approved the final manuscript.

1254

1255 **Competing interests**

1256 The authors declare no competing financial interest.

1257

1258 **Data and materials availability**

1259 All 27 primate genome assemblies and the raw genome long- and short-read sequencing data
1260 were deposited at the National Center for Biotechnology Information (NCBI) Assembly
1261 Database (<https://www.ncbi.nlm.nih.gov/assembly/>) and the Sequence Read Archive
1262 Database (<https://www.ncbi.nlm.nih.gov/sra/>) under the accessible BioProject accession
1263 codes: PRJNA785018 and PRJNA911016. We have uploaded all genome annotation GFF
1264 files to the figshare database (DOI: <https://doi.org/10.6084/m9.figshare.21692894.v1>). The
1265 positively selected genes and their sequence alignments also were uploaded to the public
1266 Dryad dataset (DOI: <https://doi.org/10.5061/dryad.8w9ghx3qj>).

1267

1268 **Supplementary Materials**

1269

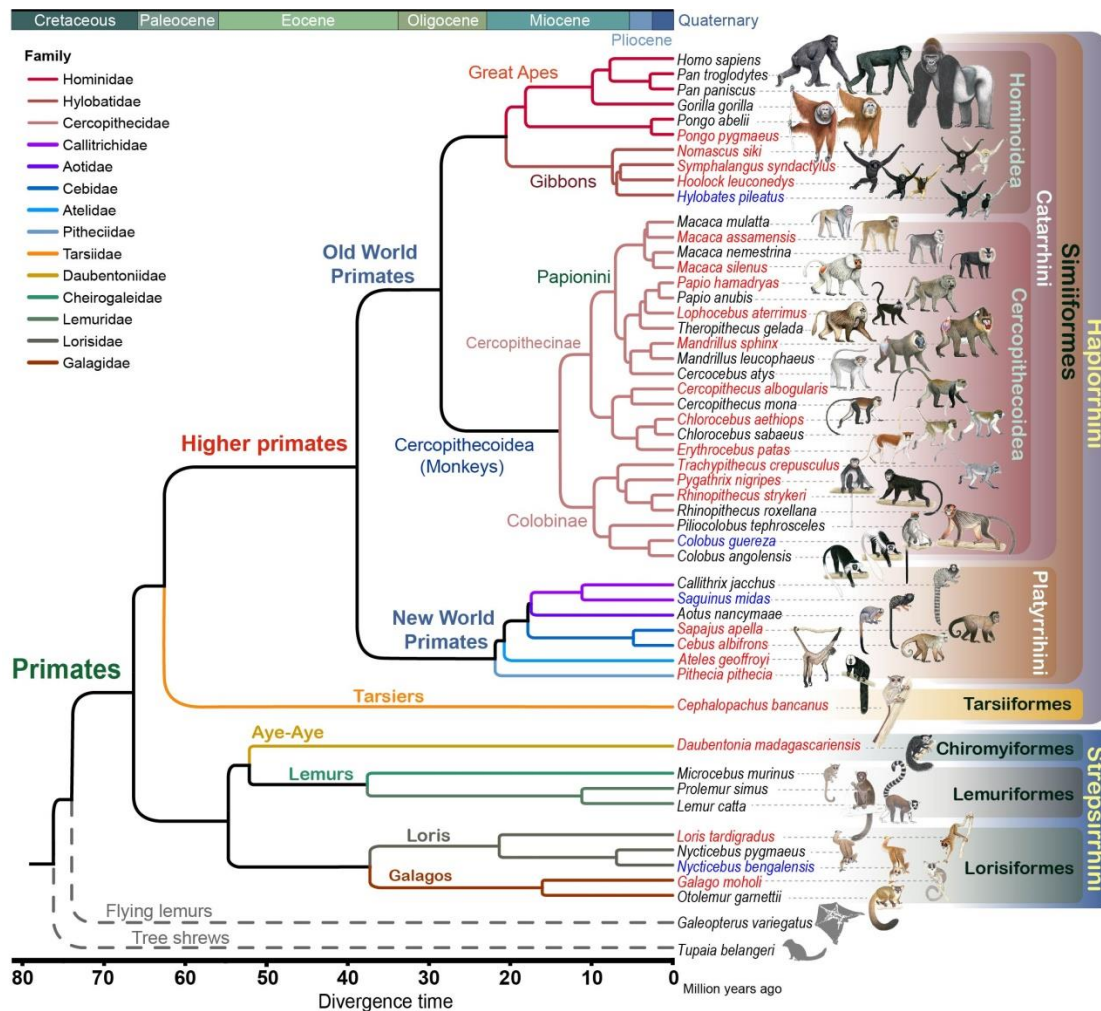
1270 Materials and Methods

1271	
1272	Figs. S1 to S39
1273	
1274	Tables S1 to S42
1275	
1276	References (158-228)

1277 **Figure legends**

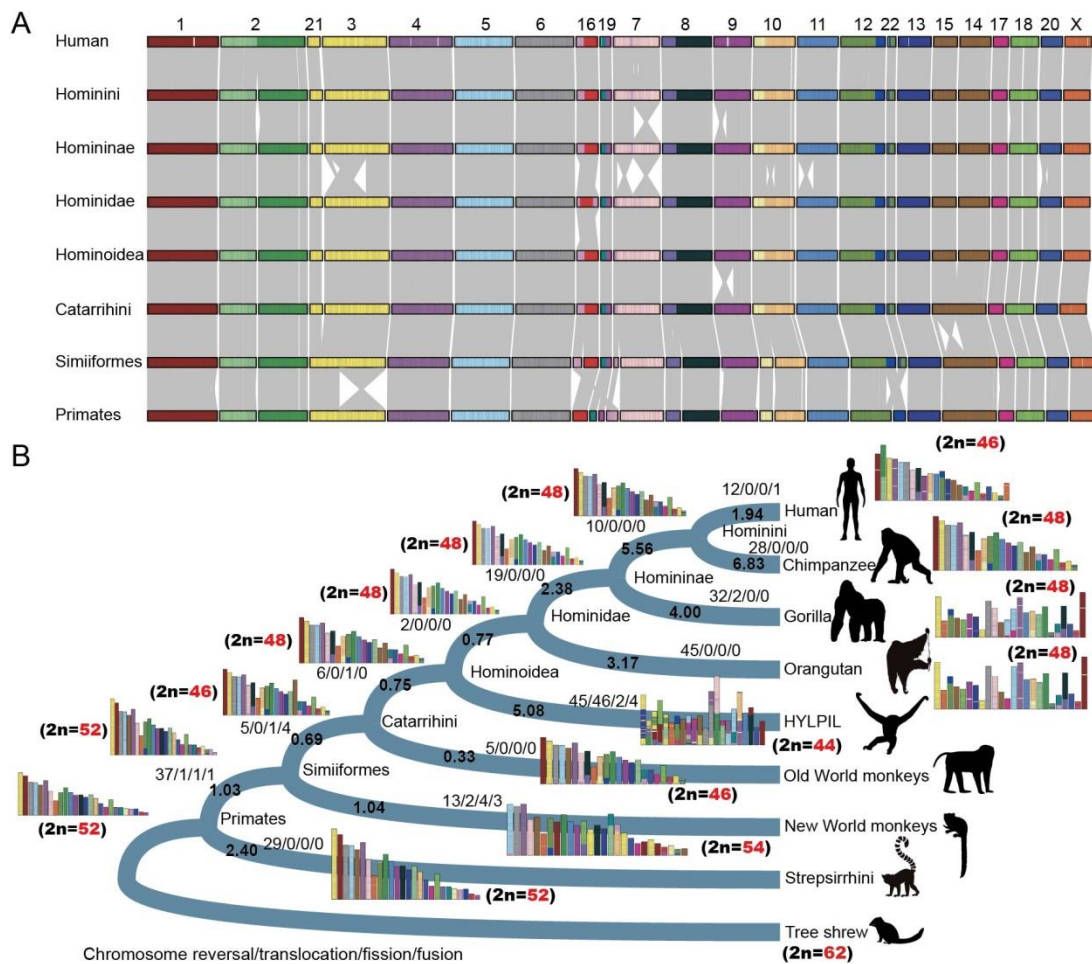
1278

1279 **Fig. 1. Genomic phylogeny of primates.** The maximum likelihood method was used
 1280 to infer the primate species tree from whole-genome sequences across 52 species
 1281 including 50 primate species and two outgroup species (Sunda flying lemur and
 1282 Chinese tree shrew) with 100 bootstraps under a GTR+GAMMA model. The
 1283 divergence time was estimated using fossil calibrations (Fig. S11) and the MCMCtree
 1284 algorithm. The red and blue species names represent those genomes newly produced in
 1285 this study. The genomes of the species marked in blue were assembled at the
 1286 chromosome level. The genomes of the species marked in black were downloaded from
 1287 the NCBI and Ensembl databases (table S8). Monkey pictures are copyrighted by
 1288 Stephen D. Nash/IUCN/SSC Primate Specialist Group, and are used in this study with
 1289 their permission.
 1290



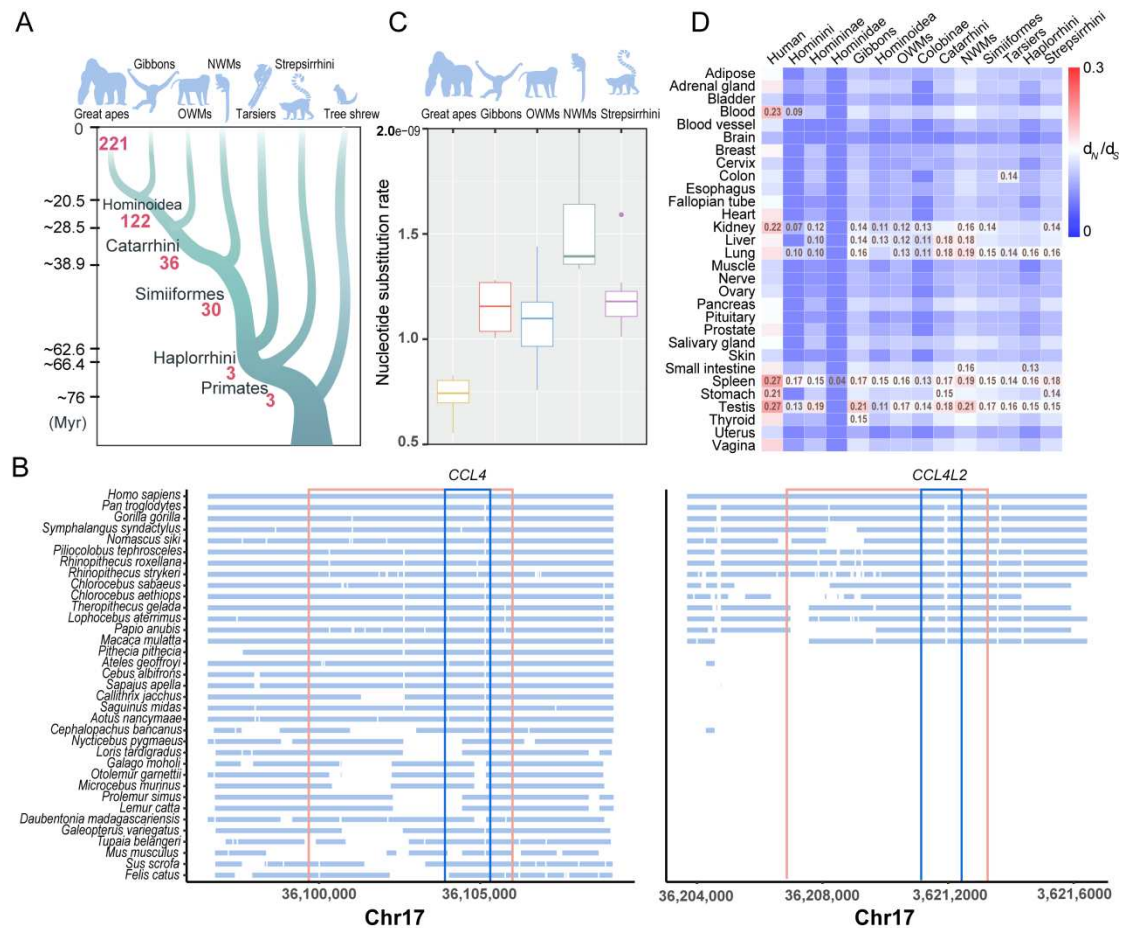
1291

1292 **Fig. 2. Reconstruction of primate ancestral chromosomes.** (A) Chromosome
 1293 evolution patterns from the primate common ancestral lineage leading to the human
 1294 lineage. Chromosomes are colored on the basis of human homologies. (B) Karyotype
 1295 evolution and genome rearrangement. The rates of genomic rearrangement are
 1296 highlighted in black bold font. Chromosome variations from ancestral nodes to derived
 1297 branches are shown by pathways including chromosome reversal, translocation, fission
 1298 and fusion events (shown in Fig. 2B by the number, e.g.,
 1299 reversal/translocation/fission/fusion). ‘HYLPIL’ represents the gibbon *Hylobates*
 1300 *pileatus*, the genome of which was assembled at the chromosome level.
 1301



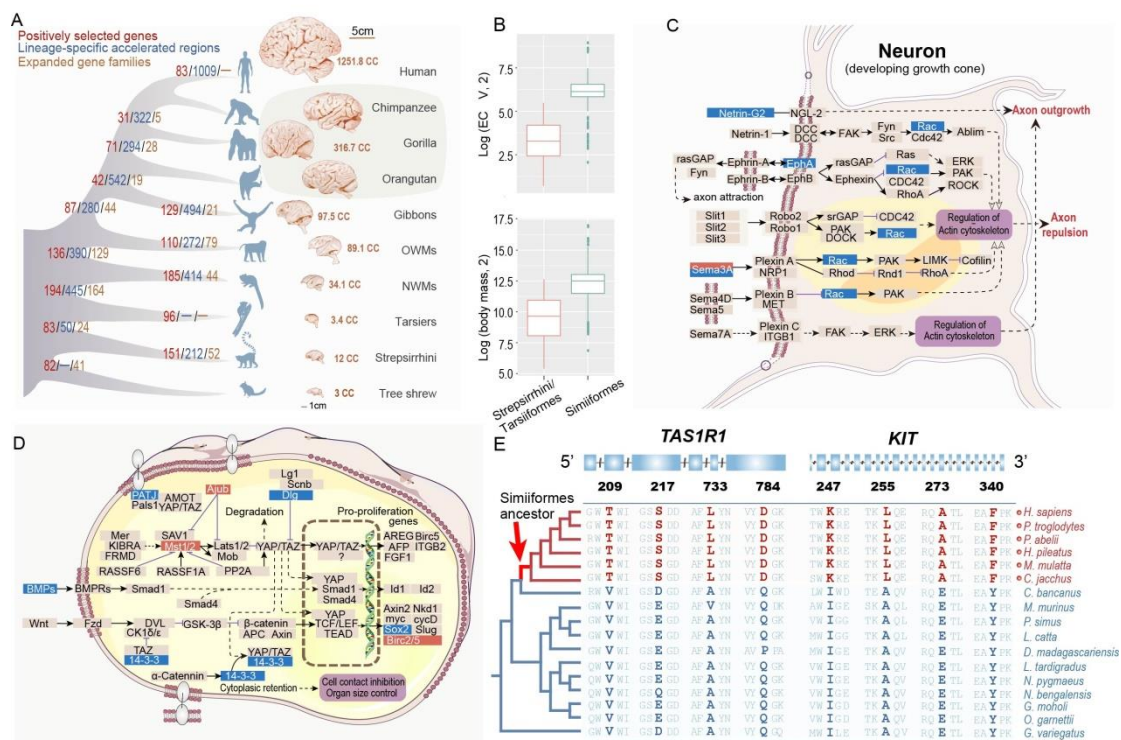
1302

1303 **Fig. 3. Structural evolution in primate genomes.** (A) Evolutionary pattern of lineage-
 1304 specific segmental duplications in primates. The numbers of lineage-specific segmental
 1305 duplications are given in red. The largest number of segmental duplications was found
 1306 in the great ape lineage. OWMs: Old World monkeys. NWMs: New World monkeys.
 1307 (B) An example of specific segmental duplications during evolution of the genome in
 1308 Catarrhini. A gene pair overlapping the segmental duplication (*CCLA*, left; *CCL4L2*,
 1309 right) is associated with HIV susceptibility. The red and green boxes represent the
 1310 segmental duplication region and the overlapping gene pair, respectively. (C) The
 1311 substitution rates across five evolutionary branches in primates. OWMs: Old World
 1312 monkeys. NWMs: New World monkeys. (D) Evolutionary constraints of tissues across
 1313 diverse lineages in primates. The evolutionary constraints of tissues are shown by the
 1314 d_N/d_S median of tissue-specific expressed genes in different evolutionary nodes among
 1315 primates.
 1316



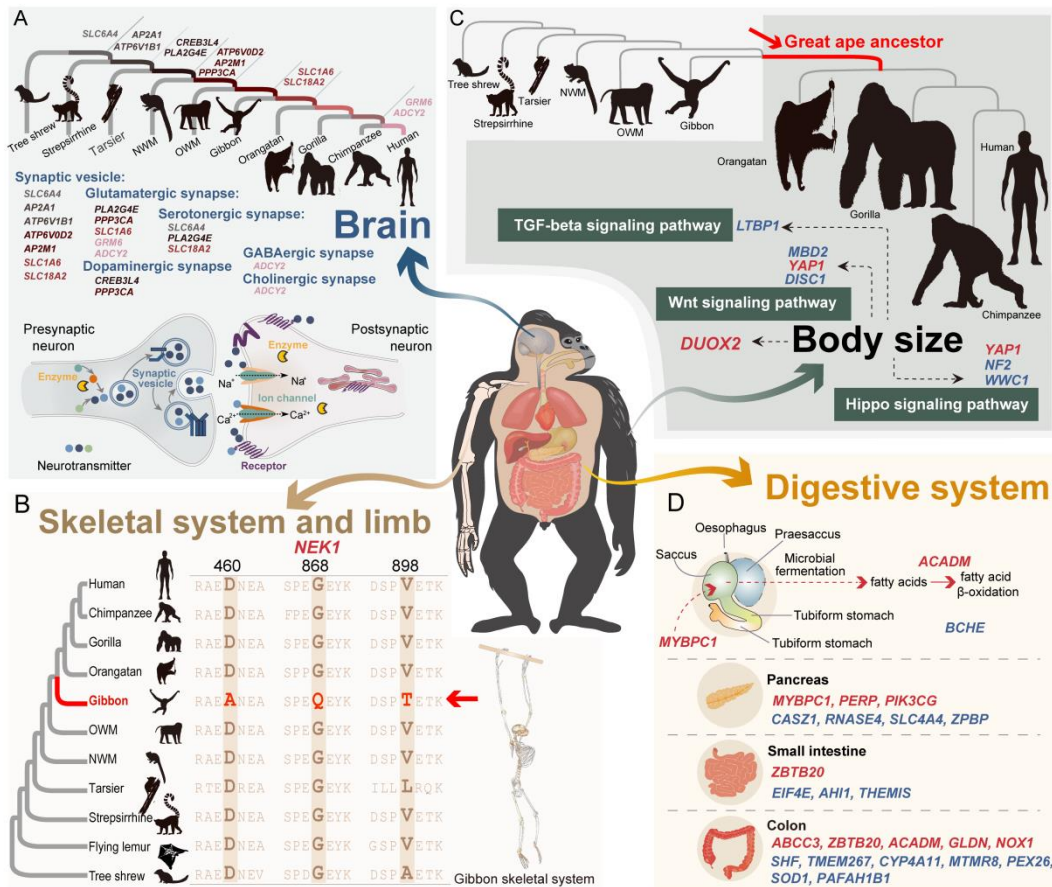
1317

1318 **Fig. 4. Genomic changes and phenotype evolution in the ancestor of the**
1319 **Simiiformes.** (A) An increased level of genomic evolutionary change including
1320 positively selected genes, lineage-specific accelerated regions, and significantly
1321 expanded gene families in the Simiiformes ancestral lineage. The brain sizes and brain
1322 structures are shown in representative evolutionary groups of primates. The brain sizes
1323 across primate and outgroup species derived from the previous studies (156, 157). Brain
1324 images are from the Michigan State Comparative Mammalian Brain Collections
1325 (www.brainmuseum.org). (B) Representative phenotype variations including brain size
1326 and body mass between Simiiformes and Strepsirrhini/Tarsiiformes. Statistical
1327 significance (*P* value) was assessed by the Mann-Whitney *U* test with *P* < 0.05. (C)
1328 Candidate genes involved in the Axon guidance KEGG pathway (hsa04360). Genes
1329 relating to genomic changes in the Simiiformes ancestral lineage are shown in this
1330 pathway. The protein product of the positively selected gene (*SEMA3B*) in the
1331 Simiiformes ancestral lineage is coloured in red. The protein products of genes
1332 associated with lineage-specific accelerated regions (*EPHA3*, *RAC1*, *NTNG2* and
1333 *SEMA3D*) are marked in blue. (D) The Hippo signaling pathway (hsa04390) – involved
1334 in organ size and body size with candidates including positively selected genes and
1335 genes associated with lineage-specific accelerated regions. The gene products for
1336 positively selected genes (*LIMD1*, *BIRC3* and *STK3*) in the Simiiformes ancestral
1337 lineage are highlighted in red, whereas the products of genes associated with lineage-
1338 specific accelerated regions (*PATJ*, *SOX2*, *BMP2*, *DLG2* and *YWHAQ*) in the
1339 Simiiformes ancestral lineage are marked by blue. (E) Multiple sequence alignments
1340 of two positively selected genes, *TAS1R1* and *KIT*, along the Simiiformes ancestral
1341 lineage. The phylogenetic position of the Simiiformes ancestor is shown by a red arrow.
1342



1343

1344 **Fig. 5. Associations between genomic evolutionary characteristics and phenotypic**
 1345 **traits in primates.** (A) Positively selected genes and genes associated with lineage-
 1346 specific accelerated regions, from the primate ancestral lineage leading to the human
 1347 lineage, involved in transport, release and receptors in neurotransmitter signaling. (B)
 1348 *NEK1* gene involved in upper limb bone development was under positive selection with
 1349 three positively selected sites in the gibbon ancestral lineage. The gibbon ancestor is
 1350 marked in red. (C) Eight positively selected genes/genes associated with lineage-
 1351 specific accelerated regions from the great ape ancestral lineage involved in the TGF-
 1352 β , Wnt and Hippo signaling pathways. (D) Positively selected genes and genes
 1353 associated with lineage-specific accelerated regions involved in the evolution of the
 1354 digestive system in the Colobinae ancestral lineage. Genes marked in red and blue
 1355 represent positively selected genes and genes associated with lineage-specific
 1356 accelerated regions, respectively, in this lineage.
 1357



1358

Fig. 6. Demographic history of non-human primates. (A) Primate species were grouped according to their biogeographic distribution (Africa, Asia and South America). The plot shows the normalized demographic history of all species within each biogeographic region. The normalized N_e was inferred by dividing the estimated value of N_e for each species at each time point by its maximum value. *Callithrix jacchus* was removed from this analysis because the genome was derived from an inbred individual. The time period from 50,000 to 20,000 years ago (late Pleistocene) is highlighted by a grey background. (B) Correlation analysis between nucleotide diversity and N_e after phylogenetic correction using the Ape library in R (<http://ape-package.ird.fr/>). N_e represents the median value of effective population size for each species 20,000 years ago. (C) Nearly half ($n=20$) of all non-human primate species experienced a continual decline in N_e over the past 3 million years (My). These include 13 critically endangered or endangered species highlighted in red. The IUCN Red List status was marked for each species in the inserted plot. CR= Critically Endangered; EN=Endangered, VU= Vulnerable; NT=Near threatened; LC=Least concern.

